ELSEVIER

Journal of Structural Geology 28 (2006) 1849–1869

JOURNAL OF STRUCTURAL GEOLOGY

www.elsevier.com/locate/jsg

What is the tectono-metamorphic evolution of continental break-up: The example of the Tasna Ocean–Continent Transition

Gianreto Manatschal [a,*], Anna Engström [b], Laurent Desmurs [c], Urs Schaltegger [d], Mike Cosca [e], Othmar Müntener [f], Daniel Bernoulli [g]

[a] *CGS-EOST, CNRS-ULP, 1 rue Blessig, Strasbourg 67084, France*
[b] *Department of Geology and Geochemistry, Stockholm University, Stockholm 106 91, Sweden*
[c] *Laboratoire de Planétologie et Géodynamique, 2 rue de la Houssinière, Université de Nantes, Nantes 44322 Cedex 3, France*
[d] *Department of Mineralogy, University of Geneva, Rue des Maraîchers 13, CH-1205 Geneva, Switzerland*
[e] *Institute of Mineralogy and Geochemistry, University of Lausanne, BFSH 2, CH-1015 Lausanne, Switzerland*
[f] *Institute of Geological Sciences, University of Bern, Baltzerstrasse 1–3, CH-3012 Bern, Switzerland*
[g] *Institute of Geology, University of Basel, Bernoullistrasse 32, CH-4056 Basel, Switzerland*

Received 25 November 2005; received in revised form 30 June 2006; accepted 14 July 2006
Available online 6 September 2006

Abstract

The break-up of continental lithosphere in magma-poor margins is accompanied by the exhumation of mantle and crustal rocks in the footwall of large-scale detachment faults. Although these structures have been described from many modern and ancient margins, little is known about how they accommodate strain and evolve in time and space during continental break-up. The Tasna Ocean–Continent Transition (OCT) in southeastern Switzerland is one of the rare examples where such detachment faults are exposed and can be observed on a kilometre scale. In this paper we describe the deformation structures and their evolution observed along detachment faults in the Tasna OCT. Our results show that continental break-up was attained by a series of detachment faults. These detachment faults accommodated extensional strain in fault zones formed by a localized core zone that is surrounded by a several tens to hundred metres wide damage zones. The core zone corresponds to the zone of highest strain and is well defined structurally by the occurrence of gouges and/or foliated cataclasites and physically by separating a hanging wall from a footwall. Deformation in the fault zones occurred under greenschist facies to seafloor conditions and within the stability field of serpentine. U/Pb ages on zircon from a garnet-bearing pegmatite cross cutting high-temperature shear zones (upper amphibolite facies and higher) provide Carboniferous ages and demonstrate that these shear zones are neither kinematically nor genetically related to the detachment faults observed in the Tasna OCT. Ar/Ar ages on phlogopite from spinel websterite suggest that mantle exhumation occurred during Middle Jurassic time. Our data show that the detachment faults observed in the Tasna OCT formed during latest rifting, post-date major thinning of the crust and onset of mantle serpentinization. These results compare well with those from the deep Iberia margin. Our observations support the idea that rifting leading to continental break-up is a multi-phase process, and that serpentinization is the consequence rather than the reason for strain localization at non-volcanic margins. Apart from the more general implications for the tectonic evolution of continental break-up, our results have some important consequences for the palaeogeographic reconstruction of certain Alpine domains and question the existence of an independent Early Cretaceous Valais ocean in the Alpine realm.

Keywords: Magma-poor rifted margin; Ocean–Continent Transition; Detachment faulting; Serpentinite gouge; Cataclasite

1. Introduction

Exhumation of mantle rocks along fault systems has been reported from slow-spreading ridges (Karson, 1990; Cannat, 1993), oceanic megamullions (e.g. Tucholke et al., 1998),

* Corresponding author. Fax: +33 3 90 24 04 02.
E-mail address: manatschal@illite.u-strasbg.fr (G. Manatschal).

0191-8141/$ - see front matter © 2006 Elsevier Ltd. All rights reserved.
doi:10.1016/j.jsg.2006.07.014

Alpine ophiolites (Decandia and Elter, 1972; Barrett and Spooner, 1977; Lagabrielle and Cannat, 1990; Lagabrielle and Lemoine, 1997) and oceanic transform faults (Bonatti et al., 1971; Bonatti, 1976). In contrast to these systems, where the exposure of the basement structures on the seafloor can be observed directly, Ocean–Continent Transitions (OCTs) of modern oceans have the disadvantage that they are usually covered by a thick pile of sediments and lie at abyssal depth. Drilling into the deep Iberia margin during ODP Leg 103 (Boillot et al., 1987) led to the discovery of the exhumation of serpentinized mantle rocks along an OCT. After ODP Leg 103, refraction seismic surveys (e.g. Discovery 215 Working Group, 1998; Chian et al., 1999; Dean et al., 2000) combined with a drilling transect across the Iberia Abyssal Plain (ODP Legs 149 and 173, Sawyer et al., 1994; Whitmarsh et al., 1998) confirmed the results obtained during ODP Leg 103 and showed that mantle rocks may be exhumed over more than 100 km across an OCT. Many authors suggested that other rifted margins in the Atlantic and elsewhere may have analogous characteristics that are at least partially similar to those described from the Iberia margin (Whitmarsh et al., 2001). Thus, exhumation of mantle rocks along detachment faults associated with serpentinization has to be considered as a major process in magma-poor margins.

In the past, processes similar to those observed at slow-spreading ridges have been proposed to explain mantle exhumation in OCTs (e.g. Sawyer et al., 1994). However, the thermo-mechanical structure of the lithosphere during continental break-up is likely to be different from that of mature Mid Oceanic Ridges (MORs). Therefore, although there are many similarities in the final structures, the associated deformation processes and their interaction with magmatism and/or serpentinization are not necessarily the same in OCTs and MORs.

Most of the studies related to the interaction between detachment faulting, mantle exhumation and serpentinization associated with continental break-up focus on the large-scale geometry of faults (Boillot et al., 1980; Reston et al., 1995, 2001; Manatschal et al., 2001), the tectono-metamorphic evolution of serpentinized peridotites (Beslier et al., 1996), the petrological and geochemical characterization of serpentinites (Gibson et al., 1996; Milliken et al., 1996; Seifert and Brunotte, 1996; Skelton and Valley, 2000), or the modelling of the serpentinization processes and their implications for the rheology of an extending lithosphere (Pérez-Gussinyé and Reston, 2001). However, few studies exist on how strain is distributed through time and accommodated during mantle exhumation, and how deformation and serpentinization interact during continental break-up. Because such studies depend on direct observations on the scale of the studied structure, they are difficult to perform in a modern margin.

Direct observation and unlimited sampling is possible in ancient OCTs exposed in collisional orogens. A remnant of such an ancient OCT is spectacularly exposed over 5 km in the Tasna nappe in the Alps of eastern Switzerland (Florineth and Froitzheim, 1994) (Fig. 1). This structure, referred to as Tasna OCT (Hölker et al., 2002b), serves as a natural analogue of modern OCTs in magma-poor rifted margins. Structural and petrological observations, combined with new radiometric ages, enable us to reconstruct the tectonic and metamorphic evolution related to mantle exhumation during continental break-up. Based on this reconstruction we discuss the relevant processes and hope to further constrain the strain evolution during continental break-up at magma-poor margins.

2. The Tasna OCT

2.1. Geological setting

The Tasna OCT is exposed along a southwest-northeast trending mountain ridge between Piz Clünas and Piz Nair in the area north of Scuol in the Engadine window in southeastern Switzerland (Figs. 1a and 2). This spectacular structure, first described by Florineth and Froitzheim (1994), is at present the only known example preserving the transition from a thinned continental crust to an exhumed subcontinental mantle undisturbed by later Alpine deformation.

The Tasna nappe, of which the Tasna OCT is a part, was emplaced during Eocene to Oligocene Alpine convergence within a north to northwest-vergent stack of thrust sheets (Fig. 1). This thrust stack is composed from top to base by: (1) Austroalpine units derived from the Adriatic, i.e. the southeastern continental margin of the Piemonte-Liguria branch of the Alpine Tethys ocean; (2) the south Penninic Arosa zone consisting of strongly tectonized remnants of the southeastern OCT of the Piemonte-Liguria basin; (3) the Tasna-Ramosch zone including the Tasna Flysch, the Tasna nappe s.str., the Ramosch zone derived from a complex realm associated with exhumed continental and mantle units from the north Alpine Tethys (see Fig. 1 and discussion in Florineth and Froitzheim, 1994); (4) the Roz-Champatsch/Stammerspitz zone, a mélange zone dominated by flysch-type sedimentary rocks including allochthonous fragments of continental and oceanic basement rocks; and (5) the Bündnerschiefer, a several kilometres thick, strongly tectonized succession of calcareous schists, containing some metabasalt bodies, classically interpreted as representing the fill of the north-Penninic Valais basin (Trümpy, 1972).

The Tasna OCT is formed by continental basement rocks and serpentinized peridotites (Piz Nair serpentinite of Florineth and Froitzheim, 1994) (Fig. 2). Triassic dolomites and Liassic limestones do not occur in the Tasna OCT, but are observed elsewhere in the Tasna nappe. In the Tasna OCT, the basement is sealed by undated dark shales, the Tonschiefer Formation, that are overlain by calciturbidites, siliciclastic sandstones and marly limestones containing breccias together spanning the time interval from Early Cretaceous to Eocene (Fig. 2b) (Hesse, 1973; Rudolph, 1982; Schwizer, 1983).

2.2. Palaeogeographic position

Staub and Cadisch (1921) interpreted the Tasna nappe as a Lower Austroalpine unit, i.e. a unit that—in modern

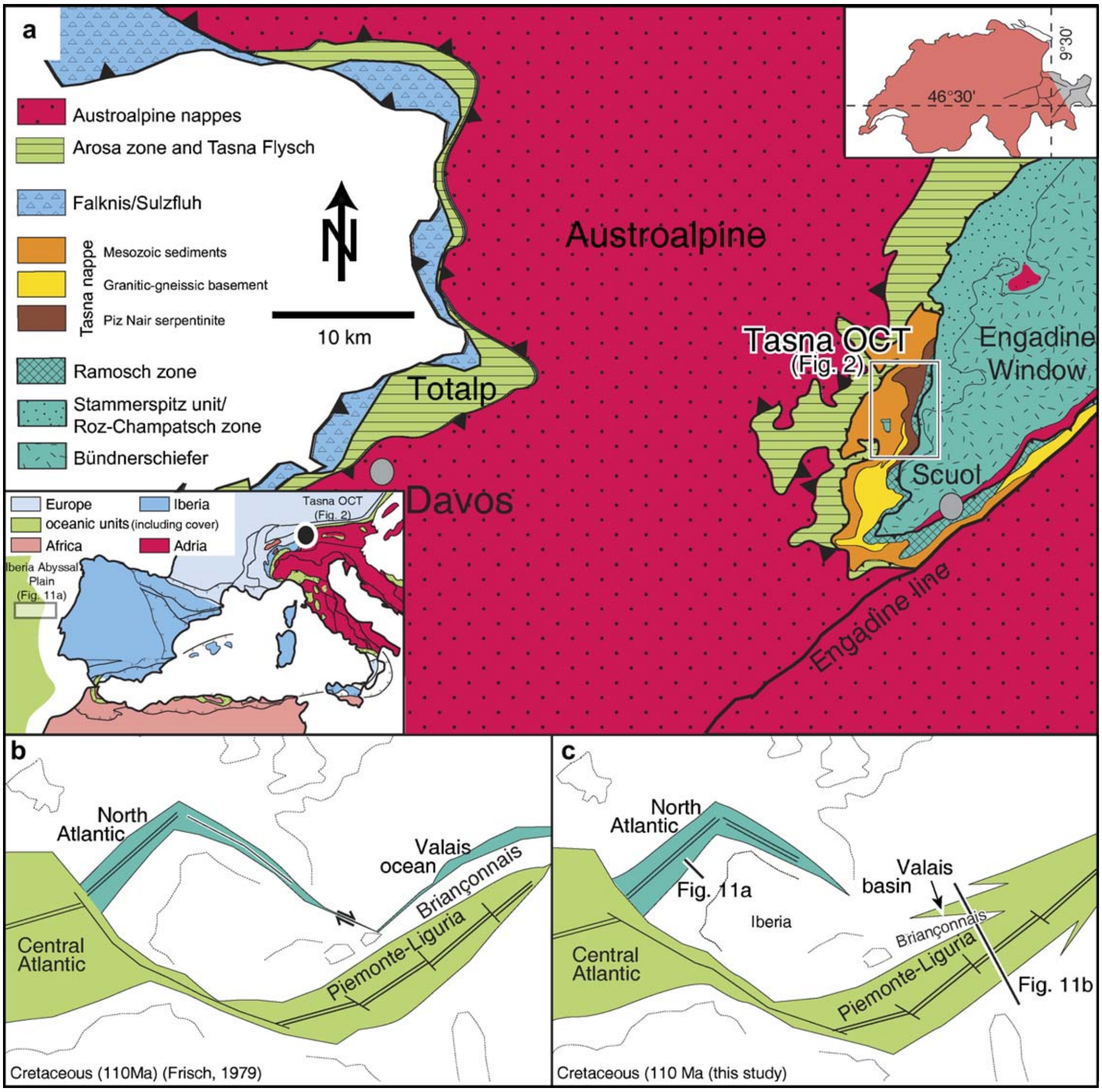

Fig. 1. (a) Tectonic map of the northwestern Grisons area in Switzerland showing the major Alpine tectonic units and the location of the Tasna OCT (modified after Trümpy, 1972; Froitzheim et al., 1994). Inset in upper right corner shows the location of the Tasna OCT in Switzerland. Inset in the lower left corner shows distribution of European/Iberian and African/Adria continental fragments in Western Europe and location of the Tasna OCT and the Iberia Abyssal Plain. (b) Palaeogeograpic reconstruction for the Alpine Tethys and adjacent areas during Late Cretaceous time (from Frisch, 1979). (c) Palaeogeographic reconstruction for the Alpine Tethys and adjacent areas as proposed in this paper.

terminology—would be derived from the former distal Adriatic margin. Trümpy (1972) interpreted the Tasna nappe to form the lateral continuation of the Falknis-Sulzfluh nappes exposed further to the west (Fig. 1) and suggested that these units came from the Briançonnais domain (Trümpy, 1980), an interpretation that is at present generally accepted. The main argument for this correlation is the similarity between the Upper Jurassic to Lower Tertiary facies associations of the Briançonnais and the Falknis-Sulzfluh-Tasna nappes.

The palaeogeographic position of the Tasna OCT is, however, not fully understood. This is mainly because of the controversy about the nature of the Valais domain situated between the Briançonnais continental fragment and the European margin (see Fig. 1b and c for more details). Frisch (1979) and Stampfli (1993) suggested the opening of an oceanic domain between Europe and Iberia/Briançonnais during Early Cretaceous time that was kinematically linked with the opening of the Bay of Biscay and the North Atlantic between Iberia and Newfoundland. In their interpretation, the Valais basin was an Early Cretaceous oceanic basin (Fig. 1b). In line with this interpretation, Florineth and Froitzheim (1994) assumed that the Tasna OCT formed the southeastern OCT of this oceanic basin, i.e. the transition between the Valais ocean and the continental Briançonnais fragment. Like Florineth and Froitzheim (1994), we place the Tasna OCT also at the northern margin of the Briançonnais fragment; however, our data do not necessarily support the opening of an independent Valais ocean during the Early Cretaceous (see Fig. 1c). Therefore, in a later part of this paper, we propose an alternative interpretation for the position of the Tasna OCT and its significance for the palaeogeographic interpretation of the Alpine domain.

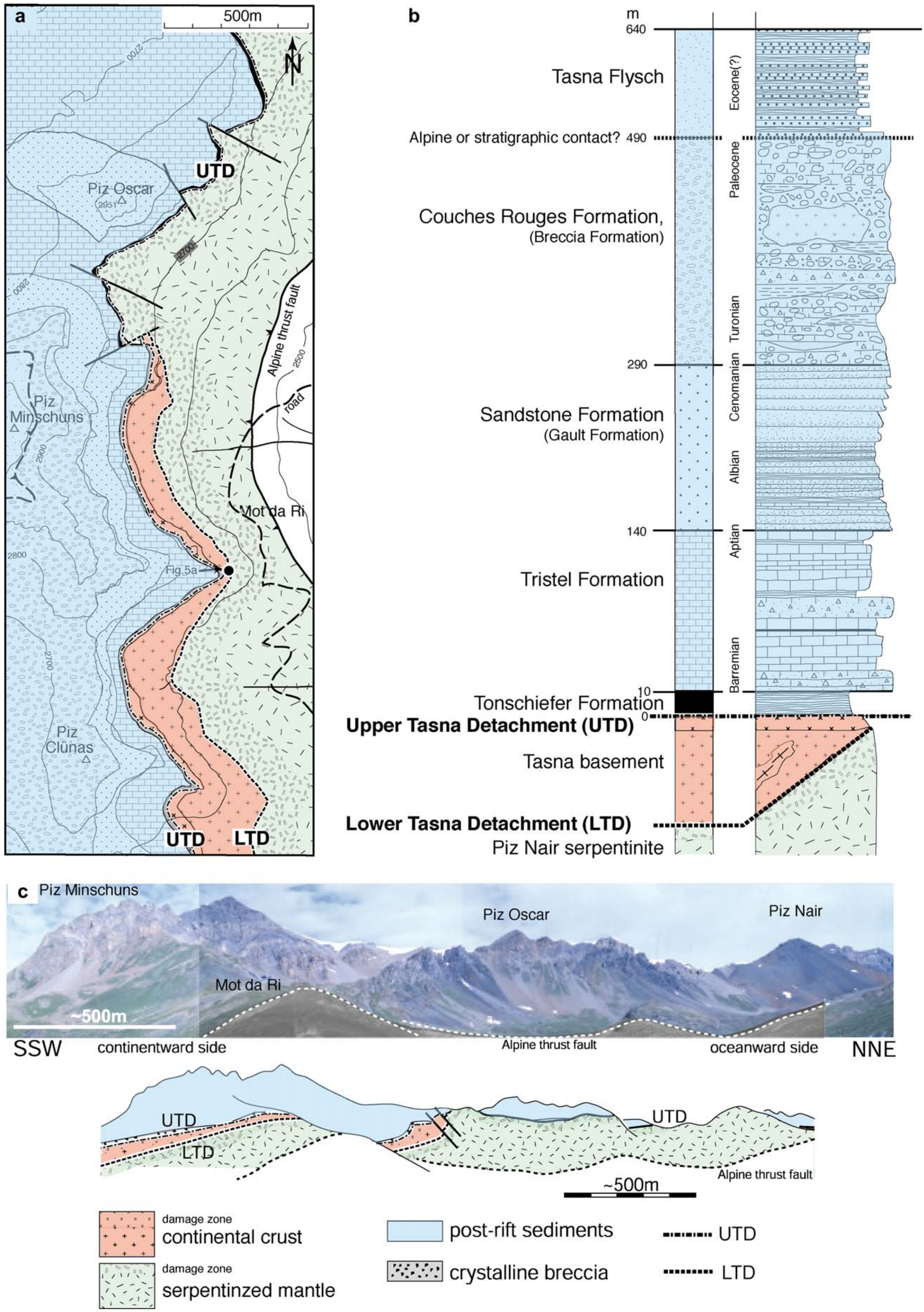

Fig. 2. (a) Geological map of the Tasna OCT and (b) stratigraphic section of the Tasna OCT (modified after Florineth, 1994). (c) Panoramic view of the Tasna OCT (view towards the northwest) and line drawing of the panorama showing the wedge of continental crust and serpentinites covered by Cretaceous to Eocene sediments (modified after Manatschal, 2004).

2.3. Present-day structure of the Tasna OCT

The structure of the Tasna OCT visible today has been described by Froitzheim and Rubatto (1998) as a wedge of continental crust bounded by two detachment faults, the Lower Tasna Detachment (LTD) separating the crustal rocks from serpentinized mantle rocks, and the Upper Tasna Detachment (UTD) which truncates the LTD and caps the basement over 4 km (Fig. 2c). Florineth and Froitzheim (1994) described the main field relationships between mantle and continental rocks forming the basement, and the overlying sediments. The most important observation is that both the continental basement and the serpentinized mantle are strongly deformed along their top and sealed by one and the same sedimentary formation, a weakly to undeformed shale, less than 10 m thick (Figs. 2a,b and 3). This thin shale layer, referred to as the Tonschiefer Formation, is overlain by the Tristel Formation, dated as Late Barremian to Early Aptian (Schwizer, 1983) (Fig. 2b). Based on the observed unconformity, covering both crustal and mantle rocks, Florineth and Froitzheim (1994) concluded that the basement structures in the mountain ridge between Piz Clünas and Piz Nair preserve an ancient transition from a continental crust to an exhumed mantle. Because the exhumed rocks in the Tasna OCT are sealed by Late Barremian sediments, they proposed that the exhumation of the mantle rocks north of the Briançonnais domain had to occur in Early Cretaceous time, an interpretation which is not corroborated by the data presented in this paper. For their part, Froitzheim and Rubatto (1998) proposed a model in which the juxtaposition of continental and serpentinized mantle rocks occurred along a lithosphere-scale detachment, the LTD being comparable to the seismically imaged S reflection

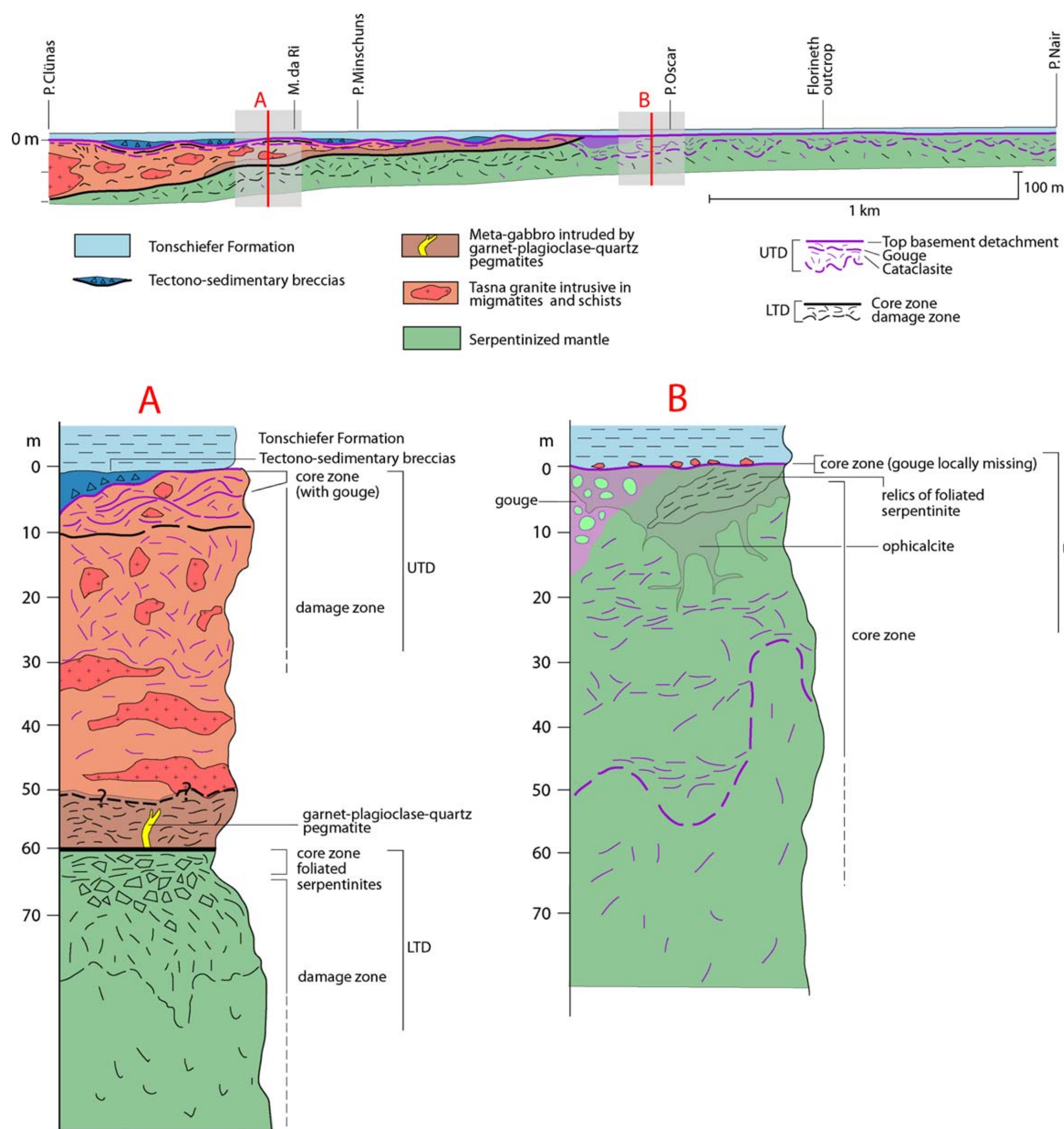

Fig. 3. Lithologies and low-temperature deformation structures in the Tasna OCT. Sections A and B show the relationships between the lithologies and the structures: A for the continental section and B for the exhumed mantle section.

in the Iberia margin (Boillot et al., 1987; Reston et al., 1995). In this paper, we will demonstrate that simple models for detachment faulting, as proposed by Froitzheim and Rubatto (1998), are incompatible with the data presented in this paper.

3. Lithologies in the Tasna OCT

The Tasna OCT comprises a wedge of continental crust that is underlain by serpentinized peridotites and unconformably capped by post-rift sediments (Fig. 3). In the following sections we describe the major rock types and present new petrological and age data.

3.1. Serpentinized mantle peridotites

The mantle rocks in the Tasna OCT are altered spinel-lherzolites with abundant spinel websterite layers and a well-defined high-temperature spinel foliation. The rocks are strongly serpentinized (>90%), but the original textures are largely preserved. Olivine is completely replaced by chrysotile/lizardite and spinel is rimmed by opaque magnetite. However, pyroxenes, rare Ti-hornblende and phlogopite are sometimes preserved. High weight percentages of incompatible elements such us sodium in clinopyroxenes indicates a fertile composition, similar to those of Malenco, the Upper Unit of the Platta nappe, Totalp and the External Ligurides (Fig. 4). A fertile composition of the Tasna peridotite is also supported by whole rock major and trace element data. Calculated temperatures from coexisting pyroxenes from lherzolites and pyroxenites indicate 900 ± 50 °C, in agreement with rather cool equilibration temperatures found in subcontinental peridotites exhumed adjacent to the continent during Jurassic rifting (Müntener et al., 2004).

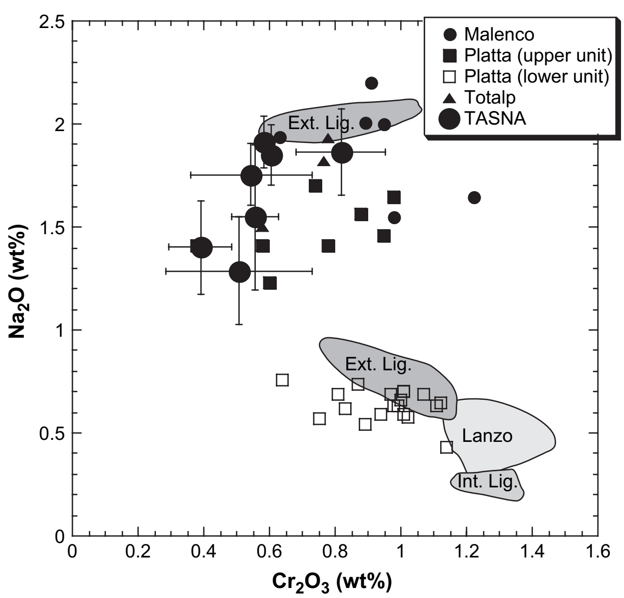

Fig. 4. Comparison of the clinopyroxene composition of the spinel lherzolite from the Tasna OCT (Na vs. Cr) with those of other ultramafic units in the Alps and the Northern Apennines (Ext.Lig, external ligurides; Int.Lig, internal ligurides). For references and locations see Müntener et al. (2004). Clinopyroxenes from the Tasna OCT are similar to the Malenco and Totalp units and the Upper Unit in the Platta nappe. All these units are interpreted as subcontinental mantle peridotites exhumed next to the continent in a former OCT (Müntener et al., 2004).

3.2. Continental crust

The continental crust in the Tasna OCT consists of two groups of rocks; one formed by variably deformed and metamorphosed migmatites that are intruded by granites and a second one formed by meta-gabbros intruded by garnet-plagioclase-quartz pegmatites (Fig. 3). The cross-cutting relationships between these two groups of rocks are shown in Fig. 3 and discussed below. The two groups of rocks record different deformation histories before their final juxtaposition and exhumation at the seafloor in Mesozoic time. The pre-rift upper crustal position for the migmatites and associated granites is indicated by their stratigraphic contact to Triassic sediments outside the considered section further to the south in the Tasna nappe (Cadisch et al., 1968). In contrast, the original position of the meta-gabbros and associated garnet-plagioclase-quartz pegmatites before onset of rifting is a matter of discussion in our paper (see Section 4.2). The meta-gabbros consist of strongly deformed igneous relics of clinopyroxene, Ti-rich hornblende, Fe–Ti oxide and (altered) plagioclase. Preliminary major element mineral chemistry of primary and metamorphic minerals indicates that the meta-gabbros are differentiated Fe–Ti gabbros (Desmurs, unpublished data). Late igneous hornblendes are ferroan pargasites, while dynamically recrystallized amphiboles can be classified as Mg-hornblende. Application of the semi-quantitative Al and Ti geothermobarometer of Ernst and Liou (1998) indicates metamorphic conditions of $T \sim 500$ °C and $p \sim 0.4$–0.8 GPa. Because the regional Alpine metamorphic conditions did not exceed greenschist facies, these conditions document a pre-Alpine history.

The meta-gabbros preserve locally a high-temperature mylonitic foliation defined by syn-kinematic recrystallization of pyroxene and plagioclase. These mylonitic domains are embedded in a matrix of dynamically recrystallized Mg-hornblende, epidote, chlorite and albitic plagioclase that partially replace the high-temperature foliation. Kinematic indicators such as σ-type clasts and shear bands show consistently a top-to-the southeast sense of shear. This is opposite to the later brittle fault zones overprinting the ductile shear zone showing a top-to-the-northwest transport direction. An important field observation is that the high-temperature mylonites are cut by weakly deformed, zircon-bearing garnet-plagioclase-quartz pegmatites that we dated with U/Pb on zircons (Fig. 5). Despite the strong oceanic alteration and later Alpine metamorphic overprint, pyrope-almandine rich garnet is still preserved.

3.3. Age determinations

3.3.1. U/Pb on zircons from the garnet-bearing pegmatite and from a meta-gabbro

Age determinations were carried out on 12 single grains and microfractions (2 to 3 grains) from two samples,

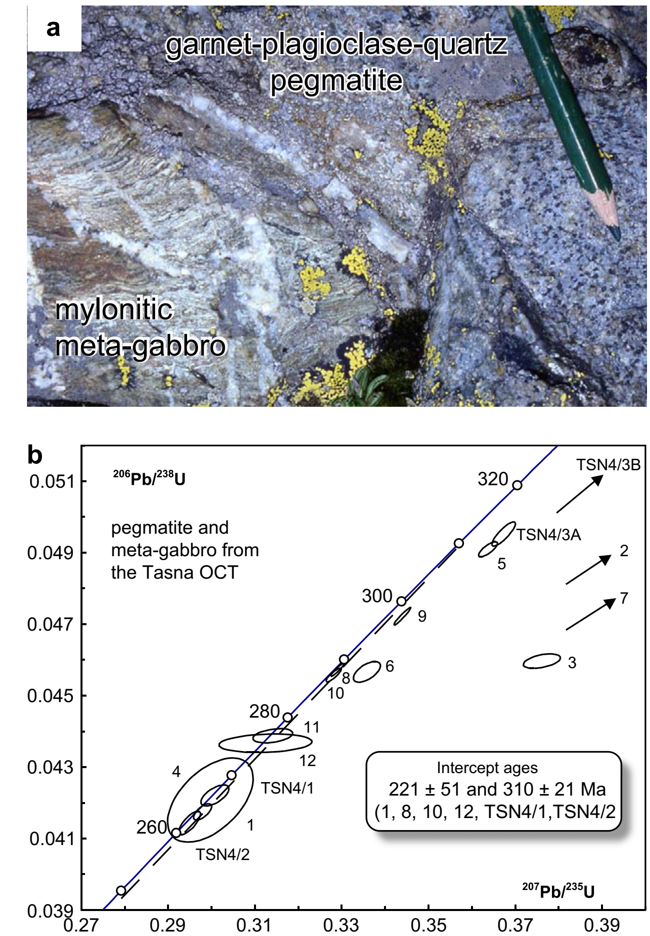

Fig. 5. U/Pb ages on zircon from the continental basement in the Tasna OCT: (a) Outcrop at Mot da Ri (for location see Fig. 2) showing a garnet-plagioclase-quartz pegmatite cutting foliated meta-gabbro; (b) Concordia plot of U/Pb zircon analyses of pegmatite and meta-gabbro from the Tasna OCT. For analytical data see Table 1.

a garnet-plagioclase-quartz pegmatite and a meta-gabbro (Fig. 5a). The age data of these zircons are all biased by both lead loss and inheritance. The data presented in Fig. 5b also include the results of Froitzheim and Rubatto (1998; TSN samples) (for analytical data see Table 1). Analyses TSN4/3B, 2, 3 and 7 point to an inherited component of Late Proterozoic age, also analyses 6, 5 and TSN4/3A are thought to be influenced by this component. The rest of the points from both samples (analyses 1, 4, 8–12) as well as TSN4/1 and 2 from Froitzheim and Rubatto (1998) define a discordia line intersecting the concordia at ages of 310 ± 21 Ma and 221 ± 51 Ma. We thus interpret these dykes to be part of the Variscan basement of the Tasna nappe that has undergone thermal alteration during rifting; i.e. during the Jurassic. A comparison of our own data with those of Froitzheim and Rubatto (1998) also demonstrates that their interpretation of a 253 Ma intrusion age for the meta-gabbro is not valid. Despite the complex zircon populations with multi-component mixing and lead loss, the intrusion of the dyke into the meta-gabbro and its mylonitization can not be related to Mesozoic exhumation, as previously suggested by Froitzheim and Rubatto (1998), but must record an older, probably Variscan or post-Variscan, i.e. Carboniferous to Permian event.

3.3.2. Ar/Ar on phlogopite

Ar/Ar dating of phlogopite separated from a spinel websterite gave two plateau segments that yielded ages of 169.1 ± 0.4 and 170.5 ± 0.4 Ma, respectively (Fig. 6) (for analytical data see Table 2). These Jurassic ages, interpreted as cooling ages, are comparable to the 160 ± 8 Ma obtained from Ar/Ar dating of phlogopite from a pyroxenite of the Totalp serpentinite (for location see Fig. 1) (Peters and Stettler, 1987). In addition to similar cooling ages, the mantle rocks in both areas also show comparable fertile mineral compositions (Fig. 4), and rather cool equilibration temperatures (around 900 ± 50 °C), suggesting that the mantle rocks from both areas represent subcontinental peridotites that were within the uppermost mantle before being exhumed during Jurassic rifting to the seafloor (Müntener et al., 2004).

3.4. The sediments of the OCT

Pre- and syn-rift sediments do not exist at the contact between basement and sediments in the Tasna OCT; however, they occur not far away in the remainder of the Tasna nappe. Polymictic breccias are observed to locally overlie the exhumed basement (Figs. 3 and 7l). These breccias include angular as well as rounded clasts of continental basement. The size of the clasts is typically less than 12 cm across. The breccias are densely packed, contain little or no matrix and the clasts are progressively flattened towards the contact with the basement rocks. Upwards, the breccias show a more open, however, chaotic framework, with a shale matrix similar to the shale forming the Tonschiefer Formation overlying the breccias and covering the Tasna OCT. Because these breccias do not show textures reminiscent of a purely tectonic or sedimentary origin, we describe them as ‘‘tectono-sedimentary breccias’’. They may result from the repeated tectonic fracturing of basement rocks, the re-assemblage of the clasts at the seafloor by gravitational movements, and deposition on a tectonically active surface and further reworking. Sub-marine erosion of the exhumed detachment may explain the local absence of fault gouges and the occurrence, in the overlying sediments, of well-rounded clasts, similar to those observed in the gouges. In a later part of this paper, we propose that the Tasna OCT may have formed a basement high that did not retain sediments. This can explain the relatively long time interval of the basement at the seafloor responsible for the intense alteration of the basement.

The tectono-sedimentary breccias are overlain by undated dark shales, the Tonschiefer Formation of Florineth and Froitzheim (1994). These sediments unconformably overlie the whole Tasna OCT and are in turn overlain by grey shales, calciturbidites and breccias forming the Tristel Formation dated as Late Barremian to Early Aptian (Schwizer, 1983) (Fig. 2b). The youngest sediments in the Tasna OCT are Aptian to Eocene siliciclastic sandstones and marly limestone

Table 1
U/Pb isotopic data of zircons from a garnet-plagioclase-quartz pegmatite and a meta-gabbro from the Tasna OCT

Number	Description[a]	Weight (mg)	No. of grains	Concentrations			Th/U[b]	Atomic ratios							Apparent ages			Error corr.
				U	Pb rad. (ppm)	Pb nonrad. (pg)		206/204[c]	207/235[d]	Error 2σ (%)	206/238[d]	Error 2σ (%)	207/206[d]	Error 2σ (%)	206/238	207/235	207/206	
Tonalite Muotta da Ri (TASNA-1)																		
1	Round, big, clrls	0.0119	2	174	7.12	1.3	0.28	2057	0.2979	0.57	0.0418	0.45	0.05175	0.42	263.7	264.7	274.3	0.68
2	Pr, clrls	0.0025	2	336	29.13	1.5	0.34	3111	0.7186	0.44	0.0860	0.37	0.06060	0.26	531.8	549.8	625.1	0.81
3	Small, pr, clrls	0.0096	3	274	12.16	22.6	0.10	353	0.3761	0.93	0.0460	0.36	0.05933	0.83	298.7	324.1	579.4	0.46
4	Round, clrls, incl	0.0061	1	77	3.92	5.1	1.09	262	0.2997	2.69	0.0421	2.29	0.05165	2.47	265.7	266.2	270.0	0.52
5	Round, clrls	0.0063	1	335	16.07	3.4	0.25	1934	0.3637	0.49	0.0491	0.35	0.05372	0.30	309.0	315.0	359.3	0.79
6	Small, round, clrls	0.0084	2	101	7.60	5.0	0.23	847	0.3358	0.76	0.0457	0.52	0.05332	0.61	287.9	294.0	342.6	0.60
7	Round	0.0132	3	275	17.59	2.6	0.26	5795	0.5356	0.39	0.0642	0.33	0.06050	0.15	401.2	435.5	621.5	0.93
Gabbro, Fuorcia da Champatsch (TASNA-2)																		
8	Spr and tips, frags	0.0068	3	938	39.27	1.4	0.04	13271	0.3290	0.38	0.0457	0.33	0.05217	0.13	288.3	288.8	292.9	0.94
9	Prism, clrls	0.0066	3	771	33.81	1.4	0.08	11348	0.3439	0.46	0.0472	0.43	0.05282	0.13	297.4	300.1	321.2	0.96
10	Spr	0.0024	2	985	41.56	2.2	0.08	3055	0.3281	0.43	0.0456	0.34	0.05221	0.22	287.3	288.1	294.8	0.86
11	Round	0.0024	1	1176	47.06	27.3	0.03	306	0.3141	1.19	0.0439	0.37	0.05190	1.11	276.9	277.3	281.1	0.36
12	Round	0.0008	1	1026	41.00	20.5	0.04	129	0.3124	2.81	0.0437	0.48	0.05188	2.77	275.5	276.0	280.2	0.17

[a] abr, abraded; anh, anhedral; clrls, colourless; euh, euhedral; frags, fragments; incl, inclusions; pr, prisms; unabr, unabraded.
[b] Calculated on the basis of radiogenic $^{208}Pb/^{206}Pb$ ratios, assuming concordancy.
[c] Corrected for fractionation and spike.
[d] Corrected for fractionation, spike, blank and common lead (Stacey and Kramers, 1975).

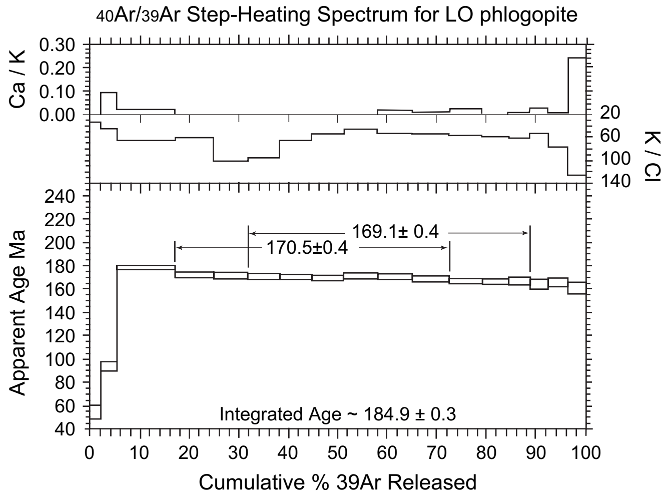

Fig. 6. Ar/Ar ages on phlogopite derived from a spinel websterite sampled at the Tasna OCT. For analytical data see Table 2.

containing megabreccias (for a more detailed description see Gürler, 1995; Bertle, 1999).

4. Deformation structures in the Tasna OCT

In this paper we mainly focus on the rift-related structures preserved in the Tasna OCT. A prerequisite to study the pre-Alpine structures is, however, that these structures can be mapped and distinguished from Alpine structures. The Alpine structures are typically related to fault propagation folds, i.e. reverse faults that cut and displace the basement/sediment contact and propagate into large-scale folds affecting the sedimentary cover. Small-scale normal faults are observed as well. Thus, deformation structures related to Alpine convergence are restricted to a few localized faults in the basement, but are more distributed in the sedimentary cover. Even though the major part of the structures observed in the basement is pre-Alpine in age, we have to admit that a diffuse Alpine overprint may have modified some of the brittle pre-Alpine structures. The following structural interpretation will mainly focus on meso- to large-scale structures that are sealed by pre-Alpine sediments along the basement-sediment contact indicating that the structures have to predate Alpine deformation as well. In a later part of this paper we propose a model that may explain why the Tasna OCT was spared from a major Alpine tectonic overprint.

4.1. Deformation structures in the serpentinized peridotite

Textures and structures in the serpentinized peridotites were studied in profiles perpendicular to the top of the serpentinized mantle in the field as well as in thin section. In the following description we distinguish between deformation structures formed under anhydrous or granulite facies conditions, here referred to as "high-temperature mantle structures" and deformation structures formed in

Table 2
Ar/Ar isotopic data of phlogopite derived from a pyroxenite from the exhumed mantle sampled in the Tasna OCT

LO Phlogopite $J = 0.00443$

Temp. (°C)	Moles ^{40}Ar ($\times10^{-14}$)	Moles ^{38}Ar ($\times10^{-15}$)	Moles ^{38}Ar ($\times10^{-17}$)	Moles ^{37}Ar ($\times10^{-17}$)	Moles ^{36}Ar ($\times10^{-17}$)	^{40}Ar*/^{39}Ar	%^{40}Ar*	Cum. %^{39}Ar	Age	$\pm1\sigma$
600	1.0571 ± 0.0277	0.7956 ± 0.0023	0.0021 ± 0.0004	−0.0001 ± 0.0002	0.0106 ± 0.0003	6.90	52.2	2.00	54.3	3.1
700	1.9692 ± 0.0300	1.2833 ± 0.0025	0.0058 ± 0.0008	0.0025 ± 0.0004	0.0132 ± 0.0005	12.12	79.3	3.23	94.3	2.0
800	11.4140 ± 0.0344	4.6561 ± 0.0087	0.0946 ± 0.0043	0.0055 ± 0.0015	0.0527 ± 0.0018	23.43	95.9	11.72	178.2	0.9
825	7.1063 ± 0.0330	3.0930 ± 0.0070	0.0366 ± 0.0062	0.0000 ± 0.0008	0.0069 ± 0.0011	22.60	98.7	7.78	172.1	1.1
850	6.3269 ± 0.0337	2.7645 ± 0.0087	0.0407 ± 0.0018	−0.0030 ± 0.0006	0.0051 ± 0.0010	22.54	98.8	6.96	171.7	1.3
875	5.7530 ± 0.0305	2.5337 ± 0.0055	0.0332 ± 0.0036	−0.0020 ± 0.0006	0.0034 ± 0.0009	22.41	99.0	6.38	170.8	1.2
900	5.8483 ± 0.0302	2.5946 ± 0.0052	0.0267 ± 0.0042	−0.0022 ± 0.0006	0.0025 ± 0.0009	22.31	99.3	6.53	170.0	1.2
925	5.7324 ± 0.0307	2.5476 ± 0.0057	0.0199 ± 0.0018	−0.0008 ± 0.0006	0.0032 ± 0.0009	22.22	99.1	6.41	169.4	1.2
950	6.1098 ± 0.0309	2.6918 ± 0.0063	0.0168 ± 0.0019	−0.0009 ± 0.0007	0.0029 ± 0.0009	22.46	99.3	6.77	171.1	1.2
975	6.4105 ± 0.0306	2.8190 ± 0.0059	0.0241 ± 0.0045	0.0024 ± 0.0007	0.0052 ± 0.0010	22.40	98.8	7.09	170.7	1.1
1000	6.7727 ± 0.0295	3.0172 ± 0.0049	0.0293 ± 0.0052	0.0019 ± 0.0008	0.0064 ± 0.0010	22.08	98.7	7.59	168.4	1.0
1025	5.7771 ± 0.0299	2.5906 ± 0.0045	0.0233 ± 0.0026	0.0022 ± 0.0006	0.0061 ± 0.0009	21.85	98.3	6.52	166.7	1.1
1050	4.7921 ± 0.0296	2.1620 ± 0.0043	0.0162 ± 0.0026	−0.0007 ± 0.0007	0.0028 ± 0.0007	21.85	98.9	5.44	166.6	1.3
1075	3.7546 ± 0.0297	1.7022 ± 0.0037	0.0108 ± 0.0009	0.0002 ± 0.0004	0.0008 ± 0.0006	21.88	99.5	4.28	166.9	1.6
1100	3.0566 ± 0.0313	1.4048 ± 0.0039	0.0061 ± 0.0004	0.0009 ± 0.0004	0.0010 ± 0.0005	21.47	99.0	3.53	163.9	1.9
1150	3.4793 ± 0.0306	1.5991 ± 0.0034	0.0114 ± 0.0015	0.0002 ± 0.0004	0.0002 ± 0.0006	21.65	99.8	4.02	165.2	1.7
1300	3.1650 ± 0.0405	1.4882 ± 0.0085	0.0123 ± 0.0006	0.0083 ± 0.0004	0.0005 ± 0.0005	21.11	99.6	3.74	161.3	2.4

Data corrected for blanks, mass spectrometer discrimination, and radioactive decay subsequent to irradiation.

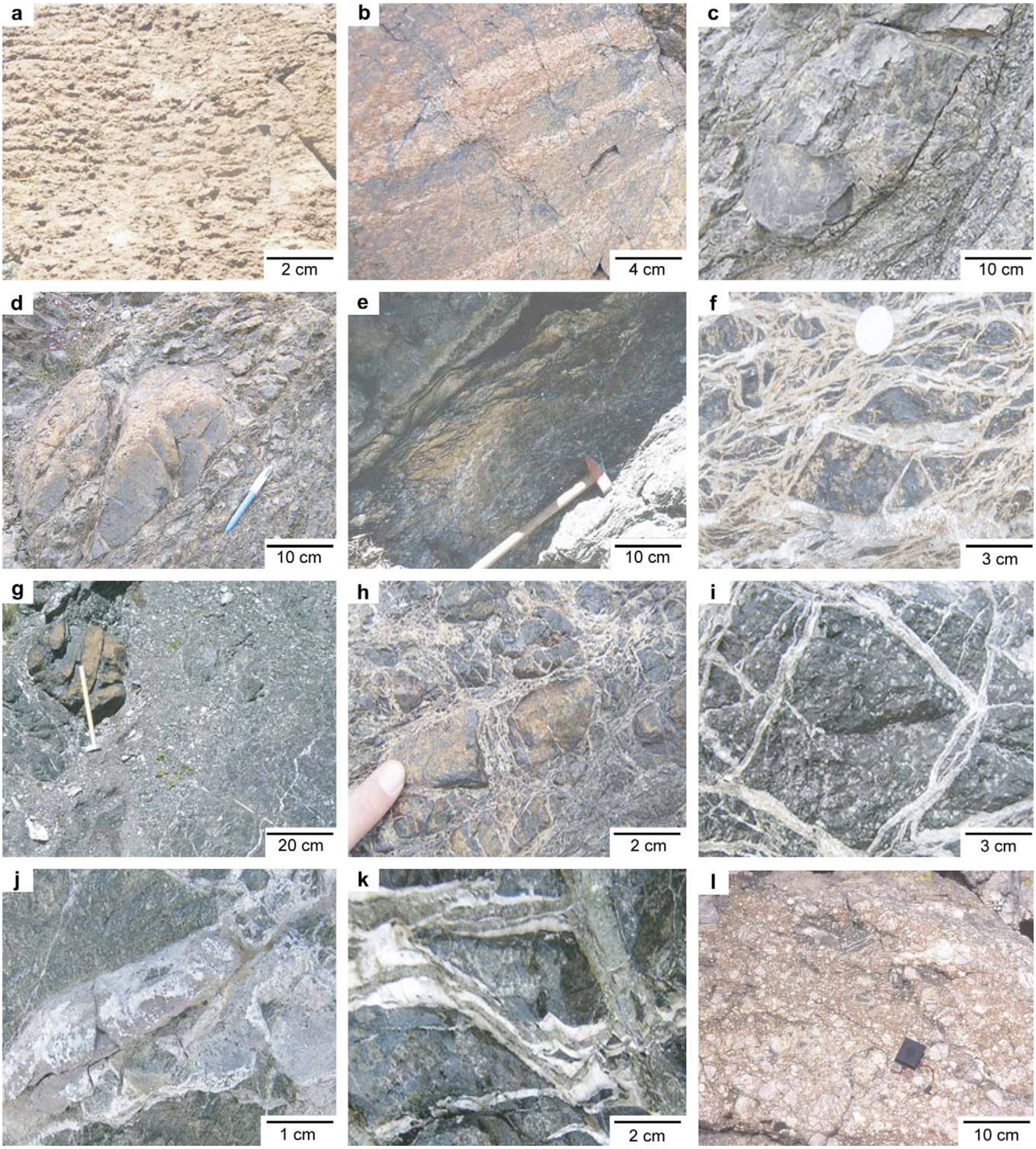

Fig. 7. Deformation structures and fault rock types observed in the exhumed mantle rocks in the Tasna OCT (for further descriptions see text). (a) spinel foliation, ∼100 m below LTD; (b) pyroxenite in serpentinized mantle peridotites, ∼100 m below LTD; (c) serpentinite cataclasite, ∼50 m below LTD; (d) serpentine clast within a pseudo-matrix of smaller serpentine clasts, ∼42 m below LTD; (e) foliated serpentinite in the core zone of the LTD; (f) foliated serpentinite cataclasite, 0.3 m below UTD; (g) serpentinite gouge, ∼15 m below UTD; (h) transitional fabric between gouge and cataclasite, ∼33 m below UTD; (i) brecciated serpentine with calcite veins, ∼14 m below UTD; (j) red microsparitic calcite vein, ∼20 m below UTD; (k) serpentine vein rimmed by calcite, ∼15 m below UTD; (l) tectono-sedimentary breccia overlying the UTD.

the presence of fluids within the stability field of serpentine minerals, here referred to as ''low-temperature mantle structures''. The distribution of the low-temperature structures is shown in Fig. 3.

4.1.1. High-temperature mantle structures

The most prominent high-temperature mantle structure is a spinel foliation that is well developed in the serpentinized peridotites (Fig. 7a). The spinel foliation is defined by elongate spinels, up to 0.5 cm long. Dip and intensity of the spinel foliation are strongly variable and no systematic trends and/or relations with the low-temperature deformation structures are observed. In the vicinity of the LTD and UTD the spinel foliation is transposed mechanically during low-temperature deformation and is oriented parallel to the major fault surface.

Mylonitic peridotites are rarely observed in the Tasna OCT. Ultra-mylonites, commonly observed in ultramafic units in the Alps, were not found.

Pyroxenites are common everywhere in the serpentinized mantle of the Tasna OCT (Fig. 7b). They can be traced over tens of metres and are generally sub parallel to, but occasionally discordant to the spinel foliation. These rocks show neither macroscopic nor microscopic evidence of a strong tectonic overprint apart from some local occurrence of elongated pyroxenes that show a preferred orientation.

4.1.2. Low-temperature structures in serpentinized mantle rocks

Mapping of the intensity and distribution of low-temperature deformation structures shows that these structures are better developed and increase in abundance towards the top of the exhumed mantle (Fig. 3). In profiles perpendicular to the top of the mantle, serpentinite cataclasites grade upwards into either foliated serpentinites (LTD) or serpentinite gouges and foliated serpentinites (UTD). Transport directions determined in the foliated serpentinites (shear bands) and gouges (mainly book-shelf faults) show a consistent top-to-the-northwest transport direction. Both gouges and foliated serpentinites occur in a well-defined narrow zone at the top of the mantle. The width of these zones ranges from several centimetres to a few metres. The zone affected by cataclastic deformation is more difficult to define. A strong and penetrative cataclastic overprint is only observed from several metres to several tens of metres below the top of the mantle (damage zone shown in Fig. 3), implying that the thickness of this zone is variable along the top of the mantle. A diffuse cataclastic overprint and localized bands of serpentinite cataclasites occur throughout the exposed mantle section. Hence, the thickness of the zone affected by brittle deformation is difficult to determine; however, the intensity of the brittle overprint seems to decrease significantly below approximately 40–70 m from the top of the mantle.

Because low-temperature deformation in serpentinites results in a wide range of structures and textures, applying a consistent terminology can be problematic. At present only few descriptions of naturally deformed serpentinites exist (Norrell et al., 1989; Hoogerduijn Strating and Vissers, 1994; Reinen, 2000). In the exhumed mantle rocks of the Tasna OCT, a wide variety of fault rocks can be distinguished, which we describe as foliated serpentinites, serpentinite cataclasites, foliated serpentinite cataclasites, and serpentinite gouges, respectively.

Serpentinite cataclasites (Fig. 7c) range from fractured serpentinites that preserve the mineralogy, structure and texture of the serpentinized lherzolite to intensely brecciated rocks forming cataclasites with sub-angular to sigmoid-shaped clasts. These rocks are typically clast-supported, exhibiting a fractal grain-size distribution. Locally, larger clasts are observed, embedded in a pseudo-matrix composed of smaller clasts of serpentinite (Fig. 7d). Where elongated, they show a weak preferred orientation parallel to the fault zone. The cataclasites show transitions into serpentinite gouges and are more frequent adjacent to high-strain zones. Although the term ‘‘foliated cataclasite’’ would adequately describe this transitional structural type, we have (for reasons of clarity) restricted our usage of this term to cataclasites that show transitions to foliated serpentinites (see below).

Foliated serpentinites and foliated serpentinite cataclasites (Fig. 7e and f, respectively) are strongly foliated serpentinites that occur in a narrow, less than a metre thick zone, along the LTD (Fig. 7e) and UTD (Fig. 7f). The foliation is defined by serpentine minerals, talc and Fe-oxides. Clasts are difficult to define within the strongly foliated serpentinites, but they occur at the transition to the serpentinite cataclasites. In contrast to the serpentinite gouges discussed below, foliated cataclasites neither show rounded clasts nor matrix-supported fabrics. The foliation clearly overprints the pre-existing cataclastic texture. This indicates that the foliation and the transposition and rotation of elongated clasts parallel to the foliation occurred in a high-strain zone after an initial stage of cataclastic deformation.

Foliated serpentinites are also observed along the UTD (Fig. 8b and c). The foliation is defined by talc, chlorite, Fe-oxides and serpentine minerals. The latter are almost completely replaced by calcite. Remnants of core-and-mantle structures and both δ- and σ-type porphyroclasts occur in these rocks. Although chlorite wraps around these clasts, the texture is reminiscent of a high-temperature peridotite-mylonite fabric (lower part in Fig. 8c). These porphyroclasts show a top-to-southeast transport direction, consistent with the transport direction obtained from shear bands. Extensive replacement of serpentine by calcite makes it difficult to decide whether the present-day foliation mimics a pre-existing high-temperature foliation or whether it formed by recrystallization under greenschist-facies conditions in the stability field of serpentine and chlorite. However, because the foliation is oblique to the top of the basement and truncated by the brittle UTD (Fig. 8b), we assume that this foliation formed under high-temperature condition and was reactivated at lower temperature before it was exhumed along the UTD to the seafloor. The foliation is overprinted by normal faults leading to book-shelf-type structures showing a top-to-the northwest transport direction.

Serpentinite gouges (Fig. 7g) are characterized by well-rounded clasts of serpentinized peridotite and serpentinites that range from several millimetres to several decimetres across and are embedded in a fine-grained serpentine matrix. In comparison with the cataclasites the matrix is more fine-grained, does not contain angular clasts and is mainly composed of serpentine minerals. The existence of transitional fabrics between cataclasites and gouges (Fig. 7 h) suggests that these two rock types are genetically linked. However,

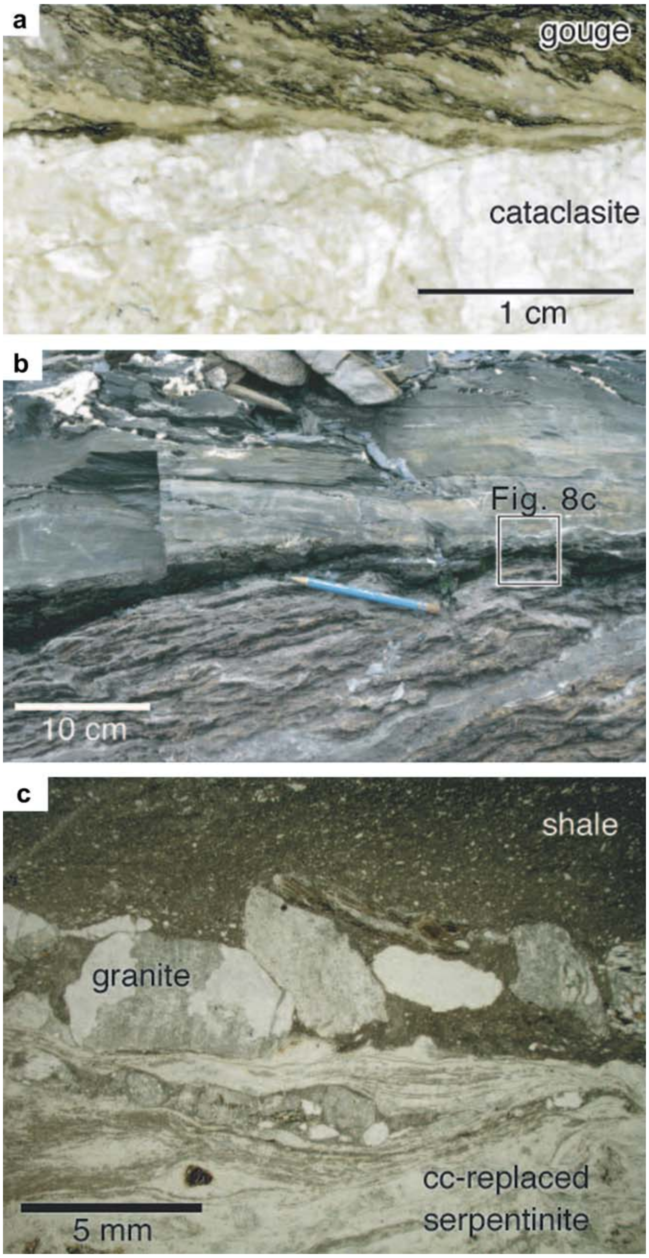

Fig. 8. Deformation structures in the continental basement and the exhumed mantle associated with the UTD. (a) Scanned image of thin section emphasizing the sharp contact between gouge and cataclasite. (b) Basement-cover contact in the Tasna OCT showing exhumed foliated mantle rocks, stratigraphically overlain by shales (e.g. Florineth-outcrop in Fig. 3). (c) Thin section of the basement-cover contact shown in (b). The section shows undeformed shales overlying a foliated serpentinite replaced by calcite. Note the imbricated and rounded clasts at the interface between sediments and exhumed mantle. The large clast to the left is granite. All clasts are continent-derived detritus. In the exhumed mantle, talc, chlorite, Fe-oxides and serpentine minerals define the foliation. The latter are almost completely replaced by calcite. Remnants of core-and-mantle structures and σ-type porphyroclasts occur in these rocks. Plane polarized light.

mature gouges do not preserve any of the characteristic features of cataclasis, such as angular clasts or clast-supported fabrics. Well-developed serpentinite gouges are only exposed in the area near Piz Oscar along the UTD (Fig. 3) where they are up to 20 m thick and stratigraphically overlain by the Tonschiefer Formation, thus of clearly pre-Alpine age. Gouges are not observed along the LTD. The contact with the underlying serpentinite cataclasite is gradual and characterized by the occurrence of calcite veins and calcite replacement that are less common in gouges. Laterally, the serpentinite gouge thins or is absent, which might be related to primary thickness variations and/or later erosion (see section B in Fig. 3).

4.1.3. Veins and ophicalcite

Serpentine and calcite veins are common in the mantle rocks in the Tasna OCT. Serpentine veins occur throughout the serpentinized peridotite. No relation between frequency and depth could be established. Both straight and anastomosing networks are observed. The restored orientation of several, millimetre-thick, straight serpentine veins along vertical profiles indicates that the most abundant generation of serpentine veins was precipitated normal to the detachment surface suggesting a direct link between veining and exhumation. There is a late generation of serpentinite veins that cut across all other structures including the above calcite veins. We assume that these veins are unrelated to exhumation, and of Alpine origin, as suggested by Hölker et al. (2002a).

Calcite occurs as a vein mineral, as a replacement and locally as infill, e.g. in geopetal fabrics, that are filled with serpentine detritus and calcite. The association of calcite and serpentinite, referred to as ophicalcite in the literature (e.g. Lemoine, 1980; Lemoine et al., 1987), can result from different processes (Bernoulli et al., 2003). Ophicalcite occurs most commonly within the uppermost few metres of the exhumed mantle along the UTD, but calcite veins and serpentine replacement by calcite is also observed to occur within a narrow zone (<1 m) along the LTD below the continental wedge.

Calcite veins range in width from several millimetres to 15 cm and are straight, anastomosing or form networks surrounding brecciated serpentine clasts (Fig. 7i). Several generations of calcite veins can be distinguished. Light-grey veins with clasts of serpentinite are cut by reddish micro spar veins, which are most frequent within the uppermost 3 to 4 metres but are also observed 20–25 m below the top of the exhumed mantle along the UTD (Fig. 7j). Calcite is also observed to rim vein-serpentine (Fig. 7k). The complete lack of any preferred alignment of calcite crystals in the veins might suggest that calcite recrystallized very late, but serpentine veins are also observed to cut across calcite veins. Thus, serpentine recrystallization may be older, coexist or postdate the formation of calcite veins.

Replacement of serpentine minerals by calcite is very common within the uppermost few metres of the mantle exposed at the seafloor by the UTD. A particularly good example is seen in Fig. 8b. In thin section it can be observed that serpentine minerals were almost completely replaced by calcite while chlorite and iron oxides define a foliation and spinel and pyroxene form σ-type porphyroclasts (Fig. 8c).

4.2. Deformation structures in the continental basement

4.2.1. High-temperature structures

An entire range of deformation structures is preserved in the continental basement. Because Triassic pre-rift sediments, exposed south of the study area, unconformably overlie both the Tasna granite and the migmatites, the high temperature structures in these rocks must be pre-Mesozoic in age and are not discussed further in this paper.

The high-temperature mylonites in the meta-gabbros are cut by a garnet-plagioclase-quartz pegmatite dated as Carboniferous (Fig. 5). Therefore, the mylonites must be Carboniferous or older. Syn-kinematic crystal-plastic deformation of pyroxene and amphibole in these mylonites indicates that these rocks were deformed under upper amphibolite-facies conditions during or following the Variscan orogeny. Kinematic indicators such as σ-type porphyroclasts shear bands and pressure-shadow tails related to this high-temperature mylonitization show a consistent top-to-southeast sense of shear. Thus, these rocks were in a mid-crustal position before final exhumation to the seafloor in Mesozoic time. Deformation under greenschist-facies conditions (at $<400\,^{\circ}C$) is only observed in quartz-rich rocks characterized by ribbon-quartz and feldspar clasts forming typical greenschist-facies mylonitic fabrics.

4.2.2. Low-temperature structures

Brittle deformation structures are very common in the continental rocks of the Tasna OCT. Some may be Alpine in age, some, especially in the granites and migmatites, may also predate Mesozoic rifting. However, the observation that the intensity of brittle deformation increases towards the top and the base of the wedge of continental crust, clearly suggests that there is a link between low-temperature deformation structures and active deformation along the UTD and the LTD. The cataclastic overprint within the basement is manifested by the occurrence of fractures, which are related to the formation of veins and cataclasites. The veins are filled by epidote, calcite, chlorite and quartz; however, the cross-cutting relationships between the veins are difficult to establish. Epidote veins unaffected by later brittle deformation are found in the central section of the basement. Outside this zone, quartz ± calcite veins cut across epidote veins in several samples. Epidote is both pre- and syn-kinematic.

Gouges occur mainly at the top of the continental basement associated with the UTD. They form narrowly spaced anastomosing zones within cataclastically-deformed host-rocks (Fig. 3). The gouges show strong lateral thickness variations ranging from zero to several metres. The local absence of gouges along the UTD may be due to erosion during their exposure at the seafloor. The contact between gouges and cataclasites are always sharp (Fig. 8a). The texture of the gouge is characterized by rounded or ellipsoid-shaped clasts embedded in a fine-grained foliated matrix defined by the preferred orientation of muscovite, biotite and chlorite. Very fine-grained rounded clasts resulting from mechanical grinding and fluid-assisted deformation are also observed in the matrix. The occurrence of injection structures indicate that the gouge material was mechanically weak during deformation and may have been deformed under high transient fluid overpressure.

In some examples, the matrix is also observed to form pressure-shadow tails flanking the clasts or wrapping around them. Where ellipsoid-shaped clasts exist, they define an NW-SE directed lineation (Fig. 9a). Using this lineation and the

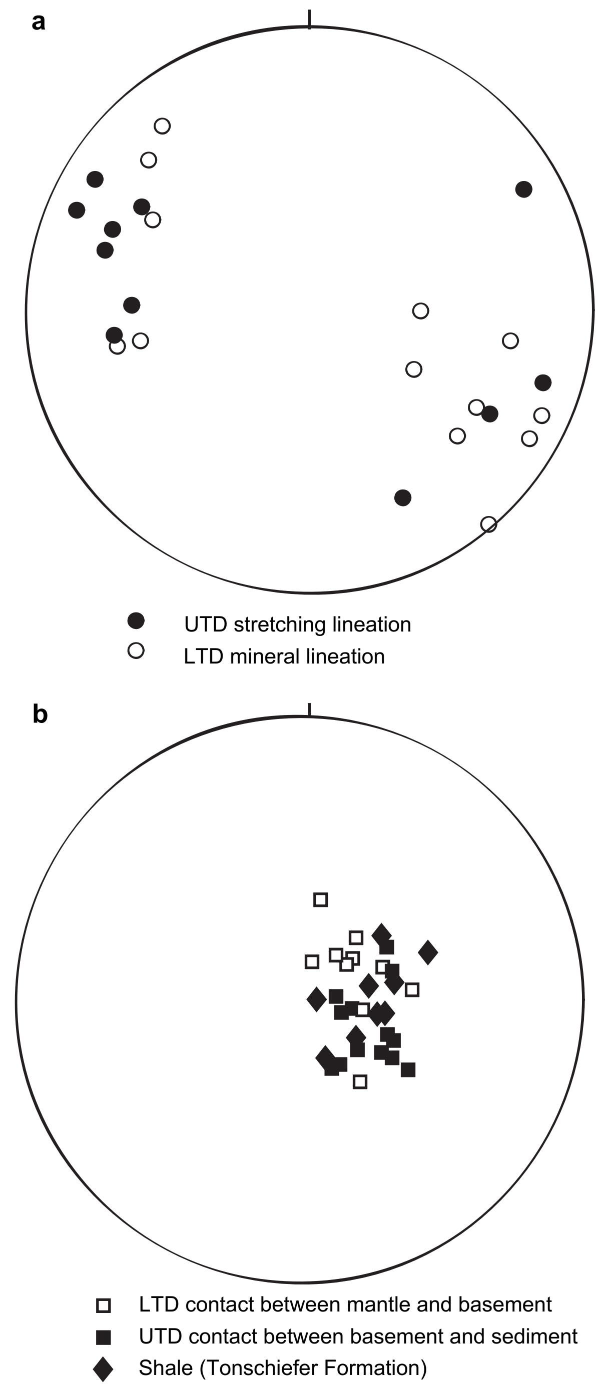

Fig. 9. Stereonet showing an equal area lower hemisphere projection. (a) Elongated clasts in gouges along the UTD defining stretching lineations and mineral lineations in foliated serpentinites and continental rocks along the LTD. (b) Pole to plane representation of the UTD and LTD surfaces displayed together with measurements of bedding within the overlying sediments sealing the OCT.

asymmetry of the clasts in the gouge, a top-to-the northwest transport direction can be determined for the UTD. Bookshelf faults, showing the same transport direction, are consistently observed to overprint the gouge zone.

4.3. Fault zone architecture of the LTD and UTD

The intra-basement LTD and the top-basement UTD form the most prominent tectonic structures within the Tasna OCT. These two structures share some common features such as: (1) a planar sub-horizontal fault architecture that is sub-parallel to the overlying sediments (Fig. 9b); (2) the same fault kinematics; and (3) a complex relationship with older high-temperature upper amphibolite-facies deformation structures. In particular the distribution of late and "cold" deformation structures shows that detachment faults, such as the LTD and UTD can not be considered as simple planes. On the contrary, they need to be described as fault zones composed of a core zone that is surrounded by a damage zone (e.g. Caine et al., 1996).

4.3.1. The core zone

The core zone is interpreted as the zone that accommodated the highest strain. It is well defined structurally by the occurrence of gouges and/or foliated cataclasites and foliated serpentinites, physically by separating hanging wall and footwall, and chemically by distinct isotopic and geochemical signatures (cf. Manatschal et al., 2000; Skelton and Valley, 2000). Although the textural transition from the damage zone to the core zone shows commonly an increase in the intensity of the deformation, on an outcrop scale, the contacts between the fault rocks forming the core (foliated serpentinites, foliated cataclasites or gouges) and the surrounding cataclasites are commonly sharp. This is particularly the case where gouges form the core zone (Fig. 8a).

The core zone of the UTD is formed, where not eroded, by gouges and/or foliated cataclasites that of the LTD by foliated cataclasites only. The lack of gouges along the LTD may be explained by the fact that the observed part of this fault was only active at deeper levels and that it was exhumed passively in the footwall of the UTD to the seafloor.

4.3.2. The damage zone

The damage zone is characterized by a strong cataclastic overprint, which did not result, except for a few cataclastic bands, in a strong strain localization. Where the brittle overprint is the strongest, the rocks are heavily fractured and form tectonic breccias. This overprint gradually decreases away from the core zone, over 40 to 70 m in the mantle, and over 5 to 10 m in the continental rocks. Thus, the heavily cataclastically overprinted zone is wider in the mantle than in the continental crust. Because the brittle deformation increases towards the detachment faults (UTD and LTD) but does not significantly affect the overlying sediments, this deformation is interpreted to be unrelated to the later Alpine overprint. However, a weak and diffuse brittle overprint related to Alpine deformation cannot be excluded.

The superposition of damage zones belonging to different detachment faults may complicate the application of the concept introduced by Caine et al. (1996). In the area of Piz Clünas for instance, two distinct damage zones related to the UTD and the LTD can be distinguished (Fig. 3). Further north, these two zones merge, resulting in a strong brittle overprint of the tip of the continental wedge. This may result in a reduction of the seismic velocities of this zone as predicted by Hölker et al. (2002a).

4.3.3. Veins

Serpentine, calcite and epidote veins occur throughout the deformed zone; they were formed before, during and after detachment faulting and can therefore not be described with the damage zone–core zone concept proposed by Caine et al. (1996). In contrast to the serpentine veins that occur throughout the deformation zone, calcite veins are more frequent in the vicinity of detachment faults. However, a comparison between the Tasna OCT and Hobby High drilled during ODP Legs 149 and 173 in the Iberia Abyssal Plain (Whitmarsh et al., 1998) shows striking differences in vein frequency and orientation patterns between the two areas. Therefore, veins cannot be considered as very reliable structural features in OCTs and do not show any particular relationship to the fault zone architecture.

5. Discussion

In the previous sections we described deformation structures in mantle and continental rocks and presented petrological and age data from the Tasna OCT. Based on these data, we first discuss the tectono-metamorphic evolution leading to continental break-up (Fig. 10). Later, we compare this evolution with that of analogue structures drilled and seismically imaged in the modern OCT in the Southern Iberia Abyssal Plain (Fig. 11a) and examine the implications of our observations for the palaeogeographic and tectonic history of the Tasna OCT (Fig. 11b).

5.1. The tectono-metamorphic evolution of continental break-up

5.1.1. Pre-rift conditions (Fig. 10a)

The pre-rift conditions of the basement rocks forming the Tasna OCT can be constrained as follows: The Tasna granite shows intrusive contacts to the migmatites to the south of the study area and the two rocks are unconformably overlain by Triassic pre-rift sediments (Cadisch et al., 1968). Thus, the migmatites and Tasna granite had to be near the surface at the onset of rifting. U/Pb ages on zircons from the metagabbros show that these rocks intruded into continental crust during or shortly after the Variscan orogeny (Fig. 5). These rocks equilibrated at $T \sim 500\,°C$, $p \sim 0.4–0.8$ GPa, i.e. at about 12 to 24 km in the middle crust.

The mantle rocks are altered spinel-lherzolites with abundant spinel websterite layers. The clinopyroxene composition of the peridotite is very similar to that of well-studied

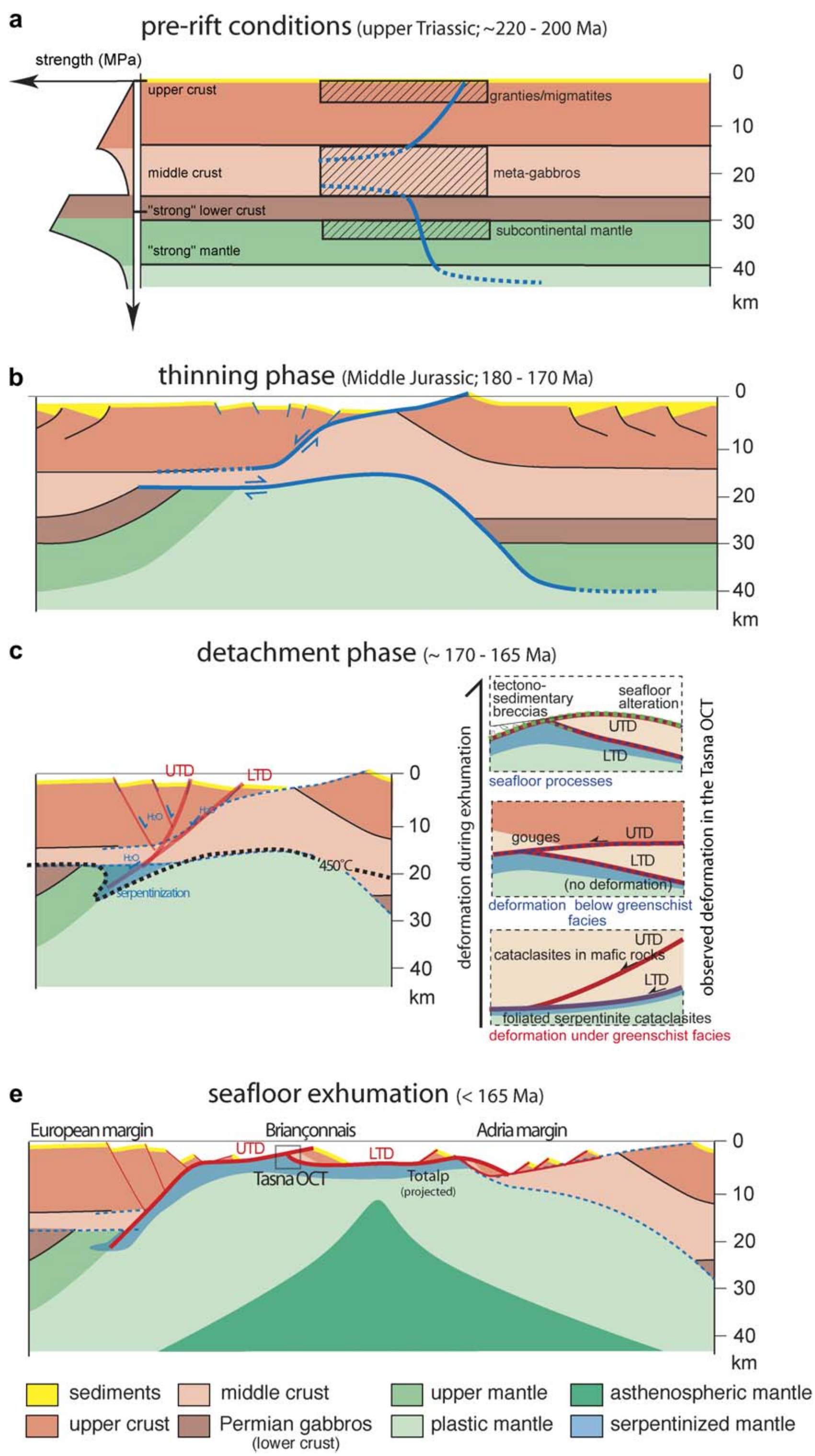

Fig. 10. Conceptual model for the tectonic evolution of the Tasna OCT showing: (a) the pre-rift conditions and the crustal levels from which the rocks in the present-day Tasna OCT are derived; (b) an early thinning phase not directly preserved in the Tasna OCT, but observed on more continentward parts of the margin (e.g. Manatschal, 2004; Lavier and Manatschal, 2006). This phase leads to the pre-detachment conditions that explain the subsequent evolution of the margin observed in the field; (c) the syn-detachment evolution with some additional steps showing the deformation observed in the Tasna OCT (this step coincides with the cooling of the mantle dated at 170 Ma; Middle Jurassic); and (d) the post exhumation history (for a more detailed discussion see Section 5.1).

examples of subcontinental mantle (e.g. Fig. 4) interpreted by Müntener et al. (2004) and Manatschal (2004) to represent the uppermost lithospheric mantle directly underlying the continental crust before onset of rifting. This interpretation is also compatible with the calculated temperatures on coexisting pyroxenes from these lherzolites and pyroxenites that are typically in the range of 900 ± 50 °C. Such temperatures suggest a rather cool equilibration for the mantle rocks.

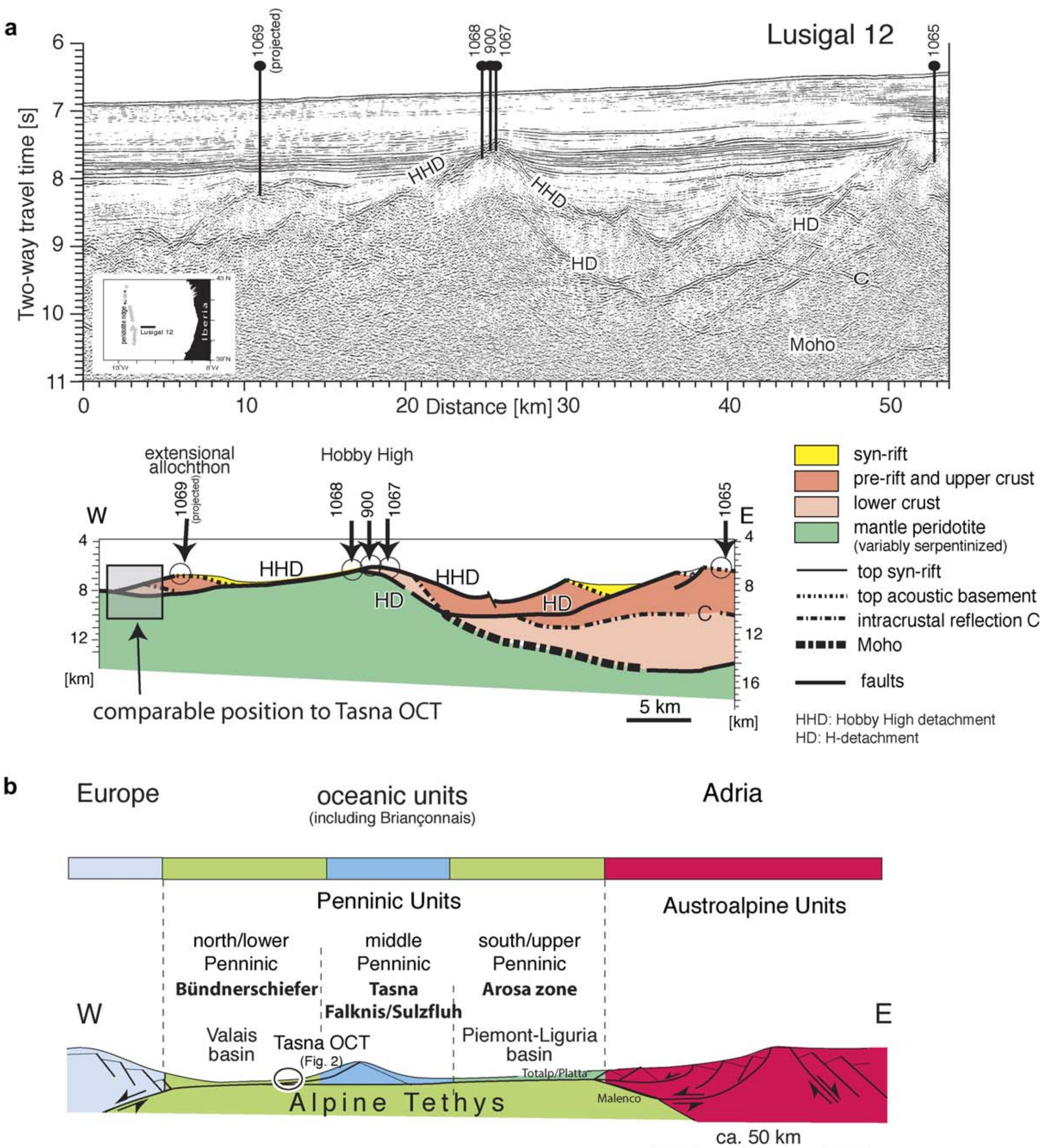

Fig. 11. (a) Lusigal 12 seismic section with ODP drill sites and geological interpretation of the depth-migrated Lusigal 12 profile (Krawczyk et al., 1996). Geological interpretation shows the distribution of mantle and crustal rocks, the existence of an allochthon (Site 1069) and of a high (e.g. Hobby High). Inset shows the position of the Lusigal 12 section in the Iberia margin. (modified from Manatschal, 2004). (b) Schematic cross section across the Alpine Tethys showing the Briançonnais/Tasna as an allochthon separating the Valais and the Piemonte-Liguria basin.

5.1.2. *Early thinning phase (Fig. 10b)*

High-temperature mylonites that formed under upper amphibolite-facies conditions (>500 °C) are observed in the meta-gabbros and, only rarely, in the mantle peridotites. In the meta-gabbros, the mylonites are cut by garnet-plagioclase-quartz pegmatites that were dated by U/Pb on zircons as Carboniferous (Fig. 5). This observation shows that the high-temperature deformation structures observed in the Tasna OCT are not related to Mesozoic rifting as proposed by Froitzheim and Rubatto (1998) but are more likely related to a late-Variscan event that seems to be widespread all over western Europe (Féménias et al., 2003). Thus, despite of the fact that the detachment faults exhumed mantle rocks during Mesozoic time to the seafloor, there is no evidence for high-temperature deformation structures of Mesozoic age related to these detachment faults. The available data show no evidence for these detachment faults being rooted at deeper levels than greenschist facies conditions. This leads to three possibilities, either that: (1) high-T structures related to rifting were eventually overprinted by low-temperature deformation structures and are not preserved; (2) the thermal gradient was extremely low and the entire crust was in the brittle field at greenschist facies or lower; or (3) detachment faults are late structures and post-date previous thinning of the crust.

The first hypothesis seems rather unlikely. If Variscan structures are still preserved, why should the younger structures be erased? However, since the lack of evidence is not a proof, we cannot exclude this hypothesis, despite of the fact that we do not find any arguments supporting the existence of high-temperature mylonitic structures related to Mesozoic detachment faulting.

Concerning the second hypothesis, Müntener et al. (2000) determined the temperature and pressure conditions at the crust-mantle boundary (T: 550 to 600 °C at 0.9 to 1 GPa) at the onset of rifting in the Alpine realm. Their results suggest a normal geothermal gradient for equilibrated continental crust that is still too high to stabilize serpentine deeper than 20 km (O'Hanley, 1996; Evans, 2004). Refraction seismic experiments from present-day OCTs show that serpentinization occurs only beneath thinned crust (e.g. Chian et al., 1999).

We therefore favour hypothesis three, suggesting that the UTD and LTD are late structures and post-date previous thinning of the crust. This is compatible with the observation that all deformation structures related to the UTD and LTD formed in the stability field of serpentine. It is also in line with the interpretation of the rift evolution on the conjugate Adriatic margin where Manatschal (2004) demonstrated that the detachment faults related to mantle exhumation are late, shallow-crustal structures. Moreover, based on large-scale reconstructions and numerical modelling of the Iberia margin Manatschal et al. (2001), Pérez-Gussinyé and Reston (2001) and Lavier and Manatschal (2006) concluded that detachment faulting related to mantle exhumation post-dates thinning of the crust to less than 10 km. Thus, in analogy with Lavier and Manatschal (2006), we assume that this early event of thinning of the crust was accommodated by a separate set of faults that soled out in middle crustal levels (Fig. 10b). The structures leading to this initial thinning of the crust are not observed in the Tasna OCT, but they are inferred to occur further continentwards (e.g. Fig. 8b in Manatschal, 2004). The previous thinning of the crust is necessary in order to explain that the LTD and UTD were able to exhume mantle without cutting down at levels hotter than greenschist facies and without exhuming lower crustal rocks in the OCT.

5.1.3. Detachment phase (Fig. 10c)

There is a close genetic link between the UTD and LTD and the distribution of low-temperature structures that is indicated by a mappable increase of their intensity towards the detachment (Fig. 3). In addition, there is a kinematically consistent relationship between small-scale and large-scale structures. Deformation structures that can be assigned kinematically to detachment faulting never have been found to form at higher temperatures than greenschist-facies conditions. The "hottest" and probably also deepest deformation structures that are not cut by the Carboniferous pegmatites and that are kinematically and spatially related to detachment faulting are quartz mylonites containing quartz ribbons and asymmetric feldspar clasts in tonalite, foliated serpentinites in ultramafic rocks and epidote and chlorite veins associated with a penetrative hydrothermal alteration in the gabbroic rocks. All these structures were strongly overprinted by later brittle deformation during their exhumation to the seafloor.

In the mantle rocks mylonitic shear zones are rare. They are neither kinematically nor geometrically related to the detachment faults. All deformation structures associated with the LTD and UTD formed in the stability field of serpentine (<450 °C and at less than 10 km depth beneath a brittle crust). The Ar/Ar ages of 169.1 ± 0.4 and 170.5 ± 0.4, respectively, obtained from phlogopite from a spinel websterite are likely to date cooling related to the exhumation of the mantle rocks in the footwall of the LTD. Therefore, we suggest that exhumation of the mantle rocks in the Tasna OCT is related to Jurassic rifting and opening of the Alpine Tethys ocean. Because the Ar/Ar ages, the clinopyroxene compositions and the calculated temperatures on coexisting pyroxenes from lherzolites and pyroxenites from the Tasna OCT are similar to those from the Totalp unit (Fig. 4) (Peters and Stettler, 1987), we suggest that these subcontinental mantle rocks share an analogous history before being exhumed during Jurassic rifting to the seafloor (Fig. 10d). While the age of exhumation of the mantle rocks in the Totalp unit is dated by Middle to Upper Jurassic radiolarian cherts, the Tasna OCT is covered by Lower Cretaceous sediments. If our hypothesis is correct, i.e. if the Ar/Ar ages date cooling and exhumation of the mantle during the Middle Jurassic, a time gap of about 40 Myr between exhumation and sealing of the peridotite basement has to be postulated. Below we test the feasibility of this hypothesis by comparing the Tasna OCT with a modern OCT seismically imaged and drilled in the Iberia Abyssal Plain.

5.1.4. Seafloor processes related to exhumed detachment faults (Fig. 10d)

The exhumation of the UTD and related mantle rocks to the seafloor is documented by their stratigraphic contact with sediments (Fig. 8b and c). As discussed before, there is a discrepancy between the age of mantle exhumation and the age of the sediments overlying the mantle of about 40 Myr. This suggests that the exhumed mantle remained exposed at the seafloor over tens of millions of years, a time scale, which is similar to that found in the Iberia OCT (Whitmarsh et al., 1998). The long seafloor exposure may explain the strong seafloor alteration and in particular the formation of ophicalcites (e.g. Abbate et al., 1980; Lemoine, 1980; Bernoulli and Weissert, 1985; Lemoine et al., 1987; Treves and Harper, 1994). Calcite veins, white calcite cements and grey or red-coloured calcareous internal sediment characterize the ophicalcites. Ophicalcites are very common in the damage and core zones of the UTD and less frequent along the LTD indicating that they are closely associated with detachment faults. However, ophicalcites always post-dates deformation and emplacement of mantle rocks at or near the seafloor, suggesting that their formation is favoured by the existence of high-permeability zones (i.e. damage zones of detachment faults) and the vicinity to the seafloor. Thus, ophicalcites may be regarded as a fingerprint of top-basement detachment faults that exhumed mantle rocks to the seafloor.

5.2. Comparison with the Iberia OCT

The most prominent structures that can be observed in the Tasna OCT are the UTD and LTD. They can be directly compared to analogous structures drilled and seismically imaged in the Iberia Abyssal Plain. Hölker et al. (2002b) proposed that the LTD is an equivalent structure to reflection HD, and the UTD is comparable to the drilled top-basement reflection HHD capping Hobby High (Fig. 11a). The remarkable similarity between the Tasna OCT and Hobby High with respect to exposed rock types, dimensions and geometry of the observed structures suggests that similar processes were involved in the formation of these structures. In the Tasna OCT, the observed structures cover only about 5 km. Thus, in order to better understand the large-scale geometry and tectonic significance of the UTD and the LTD we may compare the detachments of the Tasna OCT to the HHD and HD reflections in the Iberia Abyssal Plain (Fig. 11a). These seismic reflections, interpreted as detachment faults, can be described, on the scale of the margin, as planar, upward- or downward-concave structures. Manatschal et al. (2001) showed that they are late structures in the evolution of the margin and post-date the thinning of the crust to less than 10 km. The HD reflection (equivalent of LTD) juxtaposes rocks derived from different lithospheric levels, i.e. upper crust against lower crust and mantle (Reston et al., 1995; Manatschal, 2004). The HHD (equivalent of UTD) forms the top of the basement over tens of kilometres and is overlain by extensional allochthons and covered by sediments that are up to 60 Myr younger than the exhumation of the underlying basement (Manatschal et al., 2001). Like along the UTD, tectono-sedimentary breccias were also recovered at ODP Site 1068 from the top of the UTD and were interpreted by Manatschal et al. (2001) as the result of a conveyor-belt-type sediment accumulation whereby the exhumed footwall rocks were exposed, eroded, and re-deposited along the same active fault system. A similar interpretation may also be applicable to the tectono-sedimentary breccias overlying the UTD in the Tasna OCT.

5.3. Geological and palaeotectonic implications

Previous authors interpreted the Tasna OCT as the southern margin of the Valais ocean, a small Early Cretaceous ocean that was interpreted to be kinematically linked to the opening of the North Atlantic separating the Iberia/Briançonnais microplate from the European and North American plates (Frisch, 1979; Stampfli, 1993) (Fig. 1b). The existence of the Valais ocean remained highly disputed, on the one hand because of the badly constrained plate kinematic framework, on the other hand because of the lack of convincing field evidence. Therefore, the discovery of Lower Cretaceous sediments sealing the exhumed mantle in the Tasna OCT became one of the most important arguments in favour of the existence of an Early Cretaceous opening of the Valais ocean in the Alpine domain (Florineth and Froitzheim, 1994). However, the age of sediments overlying detachment structures in OCT's place only an upper time bracket on footwall exhumation, but a lower time bracket is given by the cooling ages of the footwall. We think that our phlogopite cooling ages of 169 to 171 Ma (errors included) are reliable and take them at face value for the exhumation of the mantle rocks to 10 km depth. In view of similar ages in the Piemonte-Liguria basin (168 ± 8 Ma, Peters and Stettler, 1987; see also Desmurs et al., 2001; Schaltegger et al., 2002), where exhumed mantle is overlain by mid-Jurassic radiolarites, we may speculate that the Tasna rocks were also exhumed to the seafloor already during the (late) Middle Jurassic. The Tasna OCT may therefore not have formed in Early Cretaceous time, as proposed by Florineth and Froitzheim (1994), but already during Middle to Late Jurassic time. Indeed, as the data from the Iberia OCT show (Fig. 11a), a long period of non-deposition and/or submarine erosion may separate mantle exhumation and post-rift sedimentation on submarine highs composed of exhumed mantle and lower crustal rocks (e.g. ODP Sites 900, 1067, 1068; Whitmarsh et al., 1998). If this is the case at Tasna, as we think, we must revise our views on the origin and the age of the Valais ocean. In the following section we propose a reinterpretation of the palaeotectonic significance of the Tasna OCT and discuss its implications for the palaeogeographic and tectonic evolution of the Alpine domain.

By and large, our data suggest that the Tasna OCT formed in the Middle Jurassic contemporaneously with the south-Penninic Piemonte-Liguria ocean (Schaltegger et al., 2002 and references therein). We think that this coincidence is not fortuitous but that there must be a connection between these more or less contemporaneous events. Although our age data are difficult to reconcile with a late opening of the Valais ocean in the Early Cretaceous, we do not question the palinspastic position of the Tasna OCT at the northwestern margin of the Briançonnais domain, as previously proposed by Florineth and Froitzheim (1994). We therefore have to look for a solution that takes into account the occurrence of Middle to Late Jurassic extension and mantle exhumation and documented Jurassic and possible Early Cretaceous magmatic activity in the Valais domain (Steinmann, 1994).

Given the 3-D segmentation of rifts and continental margins and using the Iberia margin as an analogue (Fig. 11a), we consider the possibility that (at least) the eastern tip of the Briançonnais in Grisons was an extensional allochthon that was emplaced during Middle Jurassic time in the Alpine Tethys and separated the Piemonte-Liguria basin to the southeast from the Valais basin to the northwest (Fig. 11b). According to this view, the eastern tip of Briançonnais would be comparable to the extensional allochthons occurring along the Cretaceous OCT of the Iberian Abyssal Plain that separate a window of exhumed mantle from the "true" oceanic crust to the west (see Figs. 1c and 11a).

Such a tentative interpretation, that clearly needs further exploration, questions the existence of an independent Valais Ocean coming into existence only during Early Cretaceous. This interpretation is in line with the Middle Jurassic age of mantle exhumation in both the Piemonte-Liguria basin and at Tasna and with the palaeogeographic position of the Tasna OCT on the northwestern side of the Briançonnais. It would also explain a hiatus of some tens of millions of years during which the exhumed basement was heavily affected by seafloor alteration before it was covered by Lower Cretaceous sediments. Last but not least, this interpretation may also explain why this unit escaped, in contrast to most of the adjacent oceanic and distal European units, Alpine subduction. Such an allochthon may have been accreted in front of the subduction zone within the accretionary wedge before it was thrust during Alpine collision onto more proximal parts of the European margin.

6. Conclusions

The investigation of the deformation structures in the Tasna OCT confirms hypotheses derived from drilling, seismic surveys and modelling of the present-day Iberia OCT showing that detachment faults are late shallow-crustal structures that are rather the consequence than the reason for localization of deformation in evolving margins. Our observations show that the LTD represents a classical intra-basement detachment fault that juxtaposed mantle rocks in the footwall against various types of crustal rocks in the hanging wall. The UTD caps the basement in the Tasna OCT representing an exhumed top-basement detachment fault. A comparison of the rock types and deformation structures of the Tasna OCT with those recovered at Hobby High in the Iberia Abyssal Plain shows for both locations: (1) serpentinized subcontinental mantle peridotites preserving a well-developed spinel foliation; (2) a complex continental basement composed of mafic rocks (meta-gabbros and amphibolites) preserving relics of high-temperature deformation structures that are intruded by garnet-plagioclase-quartz pegmatites dated as Variscan or post-Variscan; (3) an intense brittle overprint in mantle and continental rocks that formed under greenschist-facies to seafloor conditions showing an increase in the intensity of strain towards the detachment surfaces; and (4) the occurrence of tectono-sedimentary breccias overlying exhumed continental or mantle rocks, the absence of syn-rift sediments and a large time gap between exhumation and the emplacement of the first post-rift sediments covering the tectonically exhumed basement.

Our structural observations show that the UTD and LTD are late shallow structures that were active under greenschist to seafloor conditions and were accompanied by serpentinization of the mantle. Deformation along these detachment faults occurred in the brittle field, although, on the scale of the fault zone, deformation was localized along the core of a fault zone composed of foliated cataclasites or gouges that weakened the fault.

Last but not least, our study also resulted in the reinterpretation of the palaeogeographic setting of the Tasna OCT. We propose that the Tasna OCT is not related to the opening of a separate Valais ocean in Early Cretaceous time, but may have formed as part of a complex Middle Jurassic Alpine Tethys ocean.

Acknowledgements

We gratefully acknowledge the support of our research by the GDR Marges and the Swiss National Science Foundation (Grant 20-55284.98). We thank Niko Froitzheim for comments on an earlier version of the manuscript, and Michele Marroni and an anonymous reviewer for constructive critics of the manuscript. We thank also Annie Bouzeghaia for improving the quality of the figures.

References

Abbate, E., Bortolotti, V., Principi, G., 1980. Apennine ophiolites: A peculiar oceanic crust. Ofioliti, Special Issue (Tethyan Ophiolites) 1, 59–96.

Barrett, T.J., Spooner, E.T.C., 1977. Ophiolitic breccias associated with allochthonous oceanic crustal rocks in the East Ligurian Apennines, Italy: a comparison with observations from rifted oceanic ridges. Earth and Planetary Science Letters 35, 79–91.

Bertle, R.J., 1999. Über das Alter der Zone von Pfunds (Unterengadiner Fenster, Österreich/Schweiz). Mitteilungen der Gesellschaft für Geologie und Bergbaustudienm Österreich (Wien) 42, 119–127.

Bernoulli, D., Weissert, H., 1985. Sedimentary fabrics in Alpine ophicalcites, South Pennine Arosa zone, Switzerland. Geology 13, 755–758.

Bernoulli, D., Manatschal, G., Desmurs, L., Müntener, O., 2003. Where did Gustav Steinmann see the trinity? Back to the roots of an Alpine ophiolite concept. In: Dilek, Y., Newcomb, S. (Eds.), Ophiolite Concept and the Evolution of Geological Thought. Geological Society of America, pp. 93–110. Special Paper 373.

Beslier, M.-O., Cornen, G., Girardeau, J., 1996. Tectono-metamorphic evolution of peridotites from the ocean/continent transition of the Iberia Abyssal Plain margin. In: Whitmarsh, R.B., Sawyer, D.S., Klaus, A., Masson, D.G. (Eds.), Proceedings of the Ocean Drilling Program, Scientific Results 149. Ocean Drilling Program, College Station, TX, pp. 397–412.

Boillot, G., Grimaud, S., Mauffret, A., Mougenot, D., Kornprobst, J., Mergoil-Daniel, J., Torrent, G., 1980. Ocean–continent boundary off the Iberian margin: A serpentinite diapir west of the Galicia Bank. Earth and Planetary Science Letters 48, 23–34.

Boillot, G., et al., 1987. Tectonic denudation of the upper mantle along passive margins: a model based on drilling results (OPD Leg 103, western Galicia margin, Spain). Tectonophysics 132, 335–342.

Bonatti, E., 1976. Serpentinite intrusions in the oceanic crust. Earth and Planetary Science Letters 32, 107–113.

Bonatti, E., Honnorez, J., Ferrara, G., 1971. Peridotite-gabbro-basalt complex from the equatorial Mid-Atlantic Ridge. Philosophical Transactions of the Royal Society London 268, 385–402.

Caine, J.S., Evans, J.P., Forster, C.B., 1996. Fault zone architecture and permeability structure. Geology 24, 1025–1028.

Cadisch, J., Eugster, H., Wenk, E., 1968. Geologischer Atlas der Schweiz 1: 25000, Blatt Scuol Schuls/Tarasp, Erläuterungen. Schweizerische Geologische Kommission, Bern, 68 pp.

Cannat, M., 1993. Emplacement of mantle rocks on the seafloor at mid-ocean ridges. Journal of Geophysical Research 98, 4163–4190.

Chian, D., Louden, K.E., Minshull, T.A., Whitmarsh, R.B., 1999. Deep structure of the ocean–continent transition in the southern Iberia Abyssal Plain from seismic refraction profiles: Ocean Drilling Program (Legs 149 and 173) transect. Journal of Geophysical Research 104, 7443–7462.

Dean, S.M., Minshull, T.A., Whitmarsh, R.B., Louden, K.E., 2000. Deep structure of the ocean–continent transition in the southern Iberia Abyssal Plain from seismic refraction profiles: The IAM-9 transect at 40° 20′ N. Journal of Geophysical Research 105, 5859–5885.

Decandia, F.A., Elter, P., 1972. La zona ofiolitifera del Bracco nel settore compreso tra Levanto e la Val Graveglia (Appennino Ligure). Memorie della Società Geologica Italiana 11, 503–530.

Desmurs, L., Manatschal, G., Bernoulli, D., 2001. The Steinman Trinity revisited: mantle exhumation and magmatism along an ocean-contient transition: the platta nappe, eastern Switzerland. In: Wilson, R.C.L., Taylor, B., Froitzheim, N. (Eds.), Non-volcanic rifting of continental margins: A comparison of evidence from land and sea. Geological Society, London, Special Publications 187, 235–266.

Discovery 215 Working Group, 1998. Deep structure in the vicinity of the ocean-continent transition zone under the southern Iberia Abyssal Plain. Geology 26, 743–746.

Ernst, W.G., Liou, J., 1998. Experimental phase-equilibrium study of Al- and Ti-contents of calcic amphibole in MORB—a semiquantitative thermobarometer: American Mineralogist 83, 952–969.

Evans, B.W., 2004. The serpentinite multisystem revisited: chrysotile is metastable. International Geology Review 46, 479–506.

Féménias, O., Coussaert, N., Bingen, B., Whitehouse, M., Mercier, J.-C.C., Demaiffe, D., 2003. A Permian underplating event in late- to post-orogenic tectonic setting. Evidence from the mafic-ultramafic layered xenoliths from the Beaunit (French Massif Central). Chemical Geology 199, 293–315.

Florineth, D., 1994. Neue Beobachtungen zur Ozeanbildung und zur alpinen Tektonik in der Tasna-Decke (Randbereich zwischen Nord- und Mittelpenninikum, Unterengadin). Unpublished Diploma Thesis, ETH Zurich.

Florineth, D., Froitzheim, N., 1994. Transition from continental to oceanic basement in the Tasna nappe (Engadine window, Graubünden, Switzerland): Evidence for Early Cretaceous opening of the Valais ocean. Schweizerische Mineralogische und Petrographische Mitteilungen 74, 437–448.

Frisch, W., 1979. Tectonic progradation and plate tectonic evolution of the Alps. Tectonophysics 60, 121–139.

Froitzheim, N., Rubatto, D., 1998. Continental breakup by detachment faulting: Field evidence and geochronological constraints (Tasna nappe, Switzerland). Terra Nova 10, 171–176.

Froitzheim, N., Schmidt, S.M., Conti, P., 1994. Repeated change from crustal shortening to orogen-parallel extension in the Austroalpine units of Graubünden. Eclogae Geologicae Helvetiae 87, 559–612.

Gibson, I.L., Beslier, M.-O., Cornen, G., Milliken, K.L., Seifert, K.E., 1996. Major- and trace-element seawater alteration profiles in serpentinite formed during the development of the Iberia Margin, Site 897. In: Whitmarsh, R.B., Sawyer, D.S., Klaus, A., Masson, D.G. (Eds.), Proceedings of the Ocean Drilling Program, Scientific Results 149. Ocean Drilling Program, College Station, TX, pp. 519–527.

Gürler, B., 1995. Geologische Untersuchungen im SW-Teil des Unterengadiner Fensters: Teil I Geologie der Val Tasna und Umgebung; Beiträge zur Geologischen Karte der Schweiz, NF 166, 72 pp.

Hesse, R., 1973. Flysch-Gault and Falknis-Tasna-Gault (Unterkreide): Kontinuierlicher Übergang von der distalen zur proximalen Flyschfazies auf einer penninischen Trogebene der Alpen. Geologica et Palaeontologica. Sonderband 2, 1–90.

Hoogerduijn Strating, E.H., Vissers, R.L.M., 1994. Structures in natural serpentinite gouges. Journal of Structural Geology 16, 1205–1215.

Hölker, A., Holliger, K., Manatschal, G., Anselmetti, F., 2002a. Seismic structure of the Iberian and Tethyan distal continental margins based on geological and petrophysical data. Tectonophysics 350, 127–156.

Hölker, A., Manatschal, G., Holliger, K., Bernoulli, D., 2002b. Seismic structure and response of ocean–continent transition zones: A comparison of an ancient Tethyan and a present-day Iberian site. Marine Geophysical Researches 23, 319–334.

Karson, J.A., 1990. Seafloor spreading on the Mid-Atlantic Ridge: implications for the structure of ophiolites and oceanic lithosphere produced in slow-spreading environments, in: Malpas, J., Moores, E.M., Panayiotou, A., Xenophontos, C. (Eds.), Proceedings of the Symposium "Troodos 1987" Geological Survey Department, Nicosia, Cyprus, pp. 547–555.

Krawczyk, C.M., Reston, T.J., Beslier, M.-O., Boillot, G., 1996. Evidence for detachment tectonics on the Iberia Abyssal Plain rifted margin. In: Whitmarsh, R.B., Sawyer, D.S., Klaus, A., Masson, D.G. (Eds.), Proceedings of the Ocean Drilling Program, Scientific Results 149. Ocean Drilling Program, College Station, TX, pp. 603–615.

Lagabrielle, Y., Cannat, M., 1990. Alpine Jurassic ophiolites resemble the modern central Atlantic basement. Geology 18, 319–322.

Lagabrielle, Y., Lemoine, M., 1997. Alpine, Corsican and Apennine ophiolites; the slow-spreading ridge model. Comptes Rendus de l'Académie des Sciences. Earth and Planetary Sciences 325, 909–920.

Lavier, L., Manatschal, G., 2006. Mechanism to thin the continental lithosphere at magma poor margins. Nature 440, 324–328, doi:10.1038/nature04608.

Lemoine, M., 1980. Serpentinites, gabbros and ophicalcites in the Piedmont-Ligurian domain of the Western Alps: Possible indicators of oceanic fractures zones and of associated serpentinite protrusions in the Jurassic-Cretaceous Tethys. Archives des Sciences (Genève) 33, 103–115.

Lemoine, M., Tricart, P., Boillot, G., 1987. Ultramafic and gabbroic ocean floor of the Ligurian Tethys (Alps, Corsica, Apennines): In search of a genetic model. Geology 15, 622–625.

Manatschal, G., 2004. New models for evolution of magma-poor rifted margins based on a review of data and concepts from West Iberia and the Alps. International Journal of Earth Sciences 93, 432–466.

Manatschal, G., Marquer, D., Früh-Green, G.L., 2000. Channelized fluid flow and mass transfer along a rift-related detachment fault (Eastern Alps, southeastern Switzerland). Geological Society of America Bulletin 112, 21–33.

Manatschal, G., Froitzheim, N., Rubenach, M., Turrin, B.D., 2001. The role of detachment faulting in the formation of an ocean–continent transition: insights from the Iberia Abyssal Plain. In: Wilson, R.C.L., et al. (Eds.), Non-Volcanic Rifting of Continental Margins: A Comparison of Evidence from Land and Sea. Geological Society Special Publication 187, pp. 405–428.

Milliken, K.L., Lynch, F.L., Seifert, K.E., 1996. Marine weathering of serpentinites and serpentinite breccias, Sites 897 and 899, Iberia Abyssal Plain. In: Whitmarsh, R.B., Sawyer, D.S., Klaus, A., Masson, D.G. (Eds.), Proceedings of the Ocean Drilling Program, Scientific Results 149. Ocean Drilling Program, College Station, TX, pp. 529–540.

Müntener, O., Hermann, J., Trommsdorff, V., 2000. Cooling history and exhumation of lower crustal granulites and upper mantle (Malenco, Eastern Central Alps). Journal of Petrology 41, 175–200.

Müntener, O., Pettke, T., Desmurs, L., Meier, M., Schaltegger, U., 2004. Refertilization of mantle peridotite in embryonic ocean basins: trace element and Nd isotopic evidence and implications for crust-mantle relationships. Earth and Planetary Science Letters 221, 293–308.

Norrell, G., Teixell, A., Harper, G., 1989. Microstructure of serpentine mylonites from the Josephine ophiolite and serpentinization in retrogressive shear zones, California. Geological Society of American Bulletin 101, 673–682.

O'Hanley, D.S., 1996. Serpentinites: Records of Tectonic and Petrological History. Oxford Monographs on Geology and Geophysics 34. Oxford University Press, Oxford, UK.

Pérez-Gussinyé, M., Reston, T., 2001. Rheological evolution during extension at nonvolcanic rifted margins: Onset of serpentinization and development of detachments leading to continental break-up. Journal of Geophysical Research 106, 3961–3975.

Peters, T., Stettler, A., 1987. Radiometric age, thermobarometry and mode of emplacement of the Totalp peridotite in the Eastern Swiss Alps. Schweizerische Mineralogische und Petrographische Mitteilungen 67, 285–294.

Reinen, L., 2000. Seismic and aseismic slip indicators in serpentine gouge. Geology 28, 135–138.

Reston, T.J., Krawczyk, C.M., Hoffmann, H.J., 1995. Detachment tectonics during Atlantic rifting: analysis and interpretation of the S reflection, the west Galicia margin. In: Scrutton, R.A., Stoker, M.S., Shimmield, G.B., Tudhope, A.W. (Eds.), Tectonics of the North Atlantic Region. Geological Society London Special Publication 90, pp. 93–109.

Reston, T.J., Pennell, J., Stubenrauch, A., Walker, I., Pérez-Gussinyé, M., 2001. Detachment faulting, mantle serpentinization, and serpentinite-mud volcanism beneath the Porcupine Basin, southwest of Ireland. Geology 29, 587–590.

Rudolph, J., 1982. Tieferes Tertiär im oberen Fimbertal, Unterengadiner Fenster. Neues Jahrbuch für Geologie und Paläontologie (Monatshefte) 3, 181–183.

Sawyer, D.S., Klaus, A., Masson, D.G. (Eds.), 1994. Proceedings of the Ocean Drilling Program, Initial Reports 149, Ocean Drilling Program, College Station, Texas, 719 pp.

Schaltegger, U., Desmurs, L., Manatschal, G., Müntener, O., Meier, M., Frank, M., Bernoulli, D., 2002. Transition from a rifted continental margin to a slow spreading system: field and isotopic constraints from a Tethyan ophiolite. Terra Nova 14, 156–162.

Schwizer, B., 1983. Die Tristel-Formation, Vergleichende Untersuchung in Graubünden, Liechtenstein, Vorarlberg und Bayern. Ph. D. thesis, Bern University.

Seifert, K.E., Brunotte, D., 1996. Geochemistry of serpentinized mantle peridotite from Site 897 in the Iberia Abyssal Plain. In: Whitmarsh, R.B., Sawyer, D.S., Klaus, A., Masson, D.G. (Eds.), Proceedings of the Ocean Drilling Program, Scientific Results 149. Ocean Drilling Program, College Station, TX, pp. 497–515.

Skelton, A., Valley, J., 2000. The relative timing of serpentinisation and mantle exhumation at the ocean–continent transition, Iberia: Constraints from oxygen isotopes. Earth and Planetary Science Letters 178, 327–338.

Stacey, J.S., Kramers, J.D., 1975. Approximation of terrestrial lead isotope evolution by a two-stage model. Earth and Planetary Science Letters 26, 207–221.

Stampfli, G.M., 1993. Le Briançonnais: Terrain exotique dans les Alpes? Eclogae Geologicae Helvetiae 86, 1–45.

Staub, R., Cadisch, J., 1921. Zur Tektonik des Unterengadiner Fensters. Eclogae Geologicae Helvetiae 16, 223–285.

Steinmann, M., 1994. Ein Beckenmodell für das Nordpenninikum der Ostschweiz. Jahrbuch der Geologischen Bundesanstalt (Wien) 137, 675–721.

Treves, B.A., Harper, G.D., 1994. Exposure of serpentinites on the ocean floor: sequence of faulting and hydrofracturing in the Northern Apennine ophicalcites. Ofioliti 19, 435–466.

Trümpy, R., 1972. Zur Geologie des Unterengadins. Ergebnisse der wissenschaftlichen Untersuchungen im Schweizerischen Nationalpark 12, 71–87.

Trümpy, R., 1980. Geology of Switzerland. Part A: An Outline of the Geology of Switzerland. Schweizerische Geologische Kommission, Wepf, Basel, 1004 pp.

Tucholke, B.E., Lin, J., Kleinrock, M.C., 1998. Megamullions and mullion structure defining oceanic metamorphic core complexes on the Mid-Atlantic ridge. Journal of Geophysical Research 103, 9857–9866.

Whitmarsh, R.B., Beslier, M.O., Wallaa, P. (Eds.), 1998. Proceedings of the Ocean Drilling Program, Initial Reports 173 (CD-ROM), Ocean Drilling Program, College Station, TX.

Whitmarsh, R.B., Manatschal, G., Minshull, T.A., 2001. Evolution of magma-poor continental margins from rifting to sea-floor spreading. Nature 413, 150–154.